GEOLOGICA CARPATHICA, FEBRUARY 2023, 74, 1, 83–105 https://doi.org/10.31577/GeolCarp.2023.03

Detrital zircon geochronology of Pliocene deltaic sediments in the Marmara region (Turkey): Implication for sedimentary provenance and morphotectonic evolution

HÜSEYIN ÖZTÜRK[1,✉], İSAK YILMAZ[1], NAMIK AYSAL[1], DAVUT LAÇIN[1] and ZEYNEP CANSU[1]

[1]Department of Geological Engineering, Faculty of Engineering, İstanbul University-Cerrahpaşa, İstanbul, Turkey; ✉ozturkh@iuc.edu.tr

(Manuscript received March 30, 2022; accepted in revised form December 12, 2022; Associate Editor: Igor Broska)

Abstract: The İstanbul Pliocene deposits consist of an alternation of sand, clay, and coal in the northern part of İstanbul that characterizes a delta plain deposit on the southern coastal line of the Black Sea. The Pliocene sediments, which are located conformably on the fluvial sediments consisting of coarse clastics, are about 80 meters thick and outcrop as isolated patches in Şile in the east of the İstanbul Strait (Bosphorus) and Kısırkaya in the west. The U/Pb detrital zircon ages obtained from the sands of Kısırkaya and Şile region showed that the Pliocene deposits contain Proterozoic (2396±72–542.4±7.9 Ma), Paleozoic (540±12–258.9±5.2 Ma), Mesozoic (248.8±4.4–71.8±1.2 Ma), and Cenozoic (63±1.8–22.18±0.95 Ma) zircons derived from a piedmont plateau. Presence of the youngest Oligocene–early Miocene zircons (22.18±0.95–31.1±1.2 Ma) reveals that the source of this succession may be the Northwest Anatolia and/or northern Aegean region where magmatic rocks of the same age crop out. In addition to the zircon data in the sandy deposits, trace element geochemistry also shows that the drainage basin of the Pliocene rivers transporting clastics to the basin is located in the southwestern region of İstanbul and flowed into the Black Sea before the formation of the Marmara Sea. These rivers would have been blocked in the early Quaternary by the Marmara Sea depression, which was formed by extensional faults, the product of an approximately N–S extensional tectonic regime in the region. This tectonic regime caused the rapid uplifting of the İstanbul region and the Istranca Mountains in the north of the Marmara, and the eroded flattened areas called the Bursa–Balıkesir plateau in the south, in the form of horsts. Subsequently, before the North Anatolian fault reached the region, it formed deformation structures under the effect of dextral shear in a wide zone in the Marmara region. This tectonic regime was ended when the North Anatolian fault reached and cut the Marmara Sea region in the Latest Quaternary.

Keywords: U–Pb detrital zircon ages, Pliocene, provenance analysis, morphotectonic evolution, Marmara region

Introduction

Pliocene deltaic deposits occur in the northern part of İstanbul and consist of alternating beds of clay, sand and coal (Yeniyol 1984) located on both sides of the Bosphorus (Fig. 1). The presence of these young river sediments between the Black Sea and the Sea of Marmara is interesting because there is no palaeo-river morphology and/or drainage basin for sediment transportation into the region. According to the regional geology, the most likely provenance for sand and kaolinitic clay is the northwestern Anatolian magmatic province located south of the Sea of Marmara. If Pliocene clastics originating from this region were transported by a river system flowing into the Black Sea, the present-day İstanbul Strait should have been used and there was no Sea of Marmara during that time. Therefore, the provenance of these river sediments is important to understand an overlooked river system in a tectonically active region. These palaeogeographic findings associated with the deposition of Pliocene clastics will also contribute to the understanding of the young morphotectonic evolution of the region and the formation history of the Sea of Marmara, the Bosphorus (İstanbul Strait), the active North Anatolian Fault, and also the recent uplift history of the Uludağ–Kazdağ Mountains in the south, and the İstanbul Zone–Thrace Basin and Istranca Massif in the north.

Geology

Regional geology

The NW of Turkey consists of crustal blocks that came together during the collision of the İstanbul Zone and Istranca Massif with the Sakarya Zone, by the closure of the Intra-Pontide Ocean in the late Cretaceous, and uplifted to an erosional area in Cenozoic. The İstanbul Zone, adjacent to the Moesia platform, where the study area is located, is separated from the present-day Odesa shelf. During its southward migration along two transform faults in the late Cretaceous–Paleocene, the western Black Sea Basin was formed and then collided with the Sakarya Zone in the early Eocene (Okay 1989).

There are a number of studies on the Neogene deposition of the region and the geodynamic settings of the areas that sourced this deposition (Baykal 1942; Şengör & Yılmaz 1981; Önalan 1981a, b; Crampin & Evans 1986; Barka & Kadinsky-

(cc) BY-NC-ND

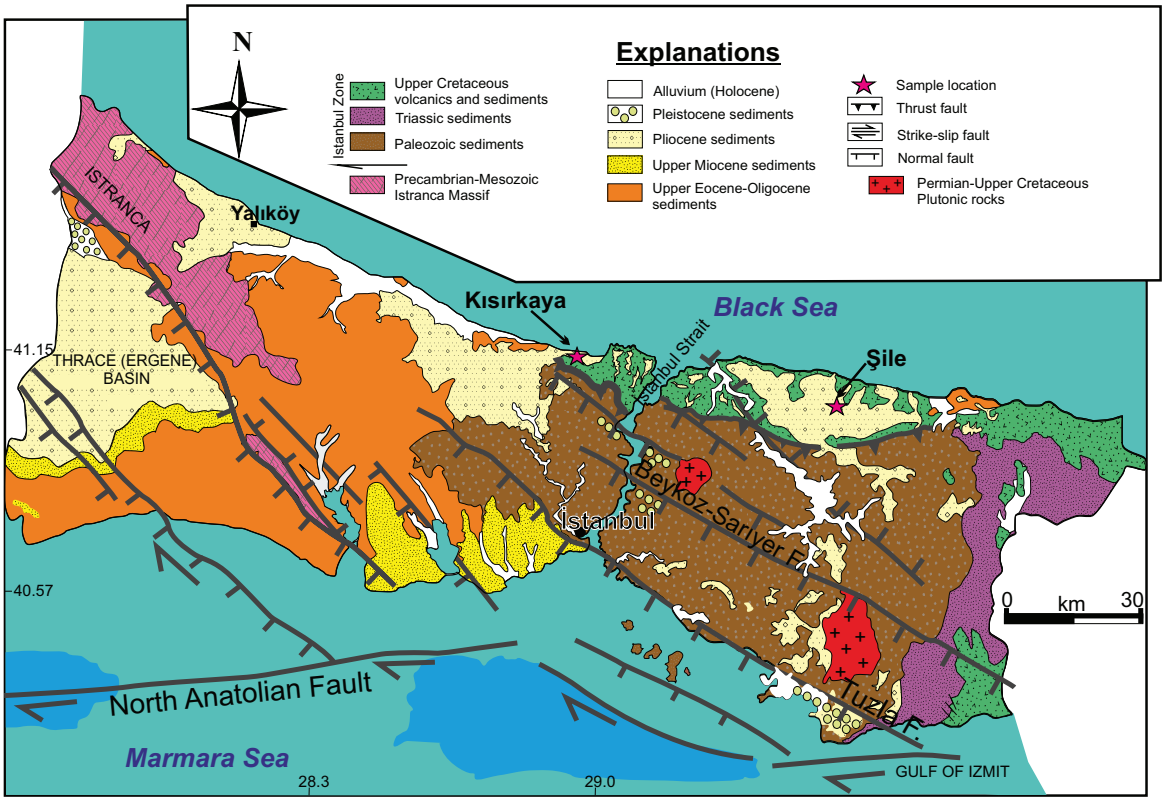

Fig. 1. Simplified geological map adopted from Şengör (2011) showing locations of the İstanbul Pliocene formations and the sampling sites.

Cade 1988; Okay 1989; Görür et al. 1997; Gedik et al. 2005; Yalçın & Yılmaz 2010; Şengör 2011; Yılmaz Şahin et al. 2014; Ülgen et al. 2018; Okay et al. 2019). The İstanbul Zone is bounded by the Black Sea in the north and the "Western Black Sea Fault" in the west by the Istranca Massif, which is represented by Paleozoic and Mesozoic magmatic and metamorphic rocks on a Precambrian basement. To the south, there are the ophiolites of the suture zone, which is thought to have passed through the Marmara Sea before the Neogene period, while the Southern Marmara region, called the Sakarya Zone is a complex region with metamorphic, magmatic, sedimentary rocks formed in the Paleozoic to Paleogene.

The Sakarya zone is separated from the Anatolide–Tauride block by the İzmir–Ankara Suture belt, a product of Neotethys closure in its south (Şengör & Yılmaz 1981; Okay et al. 1996). Anatolide–Tauride block consists of clastic and carbonate succession on a Neoproterozoic basement and lithologies which in turn were overlain by ophiolitic thrust sheets in the late Cretaceous in the north and were subjected to metamorphism and deformation during the Alpine orogeny (Şengör & Yılmaz 1981; Yılmaz et al. 2021).

The İstanbul Pliocene deposits cover the Upper Cretaceous volcano-sedimentary series (Keskin et al. 2003; Özgül et al. 2011) north of the İstanbul Paleozoic Unit (Baykal & Kaya 1963; Sayar 1964; Önalan 1981b; Yalçın & Yılmaz 2010), which consists of a passive continental margin succession extending from the Ordovician to Carboniferous. As seen from the simplified geological map (Fig. 1), there are geological formations of different ages and types around the Pliocene clastics. These include the Istranca Massif in the northwest which consists of gneiss, schist, granite, limestone, and quartzite sandstones from the Precambrian to Cretaceous age (Yılmaz Şahin et al. 2014; Natalin et al. 2016; Yılmaz et al. 2021 and references therein). The Thrace Basin sediments that reach up to nine thousand metres in thickness (Turgut & Eseller 2000; Siyako 2006; Elmas 2012) extend from the Eocene to Quaternary. Permo–Triassic basal conglomerates containing basaltic and rhyolitic intercalations unconformabe overlie the Paleozoic series, located east of İstanbul (Lom et al. 2016). Upper Permian (Sancaktepe) and Upper Cretaceous (Çavuşbaşı) granitoids were intruded into the passive margin sediments associated with northward subduction of Palaeotethys and Intra-Pontide oceanic crusts, respectively (Yılmaz Şahin et al. 2012; Aysal et al. 2018a, b). The Eocene formations unconformabe overlie the passive margin sediments of the İstanbul Paleozoic unit in the western part of İstanbul. The Miocene is represented by brackish water clays and carbonates (Şengör 2011).

İstanbul Pliocene

In general, the continent-continent collision between Africa and Eurasia caused the Tethys Ocean to be divided into two different marine areas at the end of the Eocene and

the beginning of the Oligocene. The Mediterranean was formed in the south and the Paratethys which was an Epicontinental sea that stretched from the west of China to Western Europe formed in the north. Continuous tectonic compression and uplift in the region caused the region to be divided into sub-basins (Rögl 1998; Popov et al. 2006) and geographical differentiation of these basins (Büyükmeriç 2015). The entire Aegean Region, including Western Anatolia, the Aegean Sea and the Balkan Region, became a high land during the Oligocene period (Görür et al. 1997) and began to erode effectively.

The mostly fine clastic Neogene sediments, which are the subject of the study, crop out on both sides of İstanbul in E–W trending narrow zone line in areas close to the Black Sea coast. This period presents grain size distribution and sedimentary features reflecting a deposition of energy decreasing from south to north and depending on time. It is represented by high-energy terrestrial coarse clastics (~100 m) deposited on the basement rocks in an angular unconformity, and fine clastic depositions (~80 m) that reflect the transitional environment and come on laterally and vertically.

The bottom levels of the deposition (Kayalıtepe formation), which is likely to have started in the latest Miocene, are evident with cross-bedded layers towards the north. These levels, reflecting the very high-energetic fluvial accumulation mostly cropping out in the southern parts of the region, consisting of poorly cemented, white, yellowish-brown, pink coloured sands, gravels, and conglomerates. Altered levels are yellowish red-brown and contain clay lenses and interlayers in places. It is of highly variable thickness and can reach 100 meters thick. It is lateral and vertical transitional with upper fine clastics (Meşetepe formation) cropping out in the areas close to the Black Sea coasts in the north.

These fine clastic levels, which are the subject of the study, are characterized by lenticular, silty, clayey, shale (usually bituminous), and marl layers at the base. At the top, it passes into cross-laminated quartz sands and fine pebbles with muddy dykes. It is distinctive with its grey, beige, pink, and greenish-grey colours. The lithological character and sedimentary structures of the formation reveal that the sedimentation took place in deltaic conditions, fluvial, including flood plain and isolated lake and swamp areas.

Neogene deposition seen on both sides of the Bosphorus shows differences in terms of lithological character and depositional conditions. Although radiolarite, gabbro, and serpentinitic pebbles originating from the ophiolite series are abundant in the clastics of Kısırkaya and its south, it is observed that the İstanbul Paleozoic sequence carbonates and deep marine lydite deposition fragments are dense in Şile Pliocene sands to the east.

The fact that the gravels found in coarse clastics in the west are larger and angular; the presence of scraping-impact marks in the gravels, and the presence of sole marks (burrows and fillings) reveal that they were fed by high-energetic seasonal floods and braided streams.

In addition, the orientation of the pebble long axes, imbricated pebbles, cross laminations, and asymmetric sole marks at the high-energy base levels of the deposition on both sides of the strait indicate that the transport took place from south to north. Palaeocurrent data at sandy levels reflecting the low-energetic deltaic conditions above show an irregularly oriented distribution (Özgül et al. 2011). Although there are occasional vertebrate fragments, silicified stems and leaves belonging to plants, in the sedimentation, there is no age data based on fossil coverage.

The İstanbul Pliocene consists of deltaic sediments of about 80 meters in thickness and well-bedded, close to horizontal and dipping slightly to the north in the Şile region. Clay and sand were produced from the clastic series that unconformably overlies the Cretaceous volcaniclastics. A lot of open-pit mines operate at present and open-pit sections provide excellent opportunities for geological observations, especially considering the flat topography of the region.

The Şile Pliocene sequence begins with sandy-pebbly clastics at the bottom, gradually passes into clayey-coal series in the middle, and has silty, sandy, and pebbly sediments at the top (Fig. 2). The clays are always located under layers of lignite or organic matter-rich dark greyish silty clay. Greyish kaolinitic clay layers locally include small black wood branches that indicate transportation of both clay and wood material by rivers. The clay beds consist of four economic layers and the total thickness is about 10 meters. Cross-bedding and pebble imbrication is visible in brownish sandy gravel beds with a few tens of cm thickness that are located just on top of the coal-bearing clayey zone. The Pliocene clastics are weakly cemented and include E–W striking and north-dipping syn-sedimentary normal faults (Fig. 3a, b). The uppermost light brown coloured silty sands are more than 20 meters thick and include very dense mud dykes up to 0.5 m in thickness as vertical to sub-vertical bodies (Fig. 3c). The mineralogical composition of the clay consists mainly of kaolinite, with minor illite and montmorillonite. The mineralogy of the sandy layers is composed of quartz, feldspar and minor mica. The coal beds are thin (0.2–0.7 m in thick) and have a low calorific value (<2000 Kcal) therefore a small amount of coal production occurs in the Şile region.

The Kısırkaya Pliocene series occurs in the west of the İstanbul Strait and is also located on Cretaceous volcaniclastics, similar to the Şile region. In this area, mining has been operating especially for coal and sand production since the 1900s. Hard and high calorific coal (>2500 kCal) seam-bearing Oligocene formations also occur in the eastern part of the Pliocene deposits (Çelik et al. 2017).

The Kısırkaya Pliocene sequence begins with coarse-grained clastics at the bottom and gradually passes into clay-lignite dominated fine-grained sediments, like the Şile section. Low-calorific lignite levels are located on the light grey clays, which have close to horizontal bedding. The total clay thickness at Kısırkaya is about 6 meters and the quality is lower than in the Şile region. The lignite and clay intercalated deposits are overlain by sandy sediments at the top. Contrary to the brownish Şile section, sands at Kısırkaya are greyish-light coloured (Fig. 3d). Compared to the Şile section,

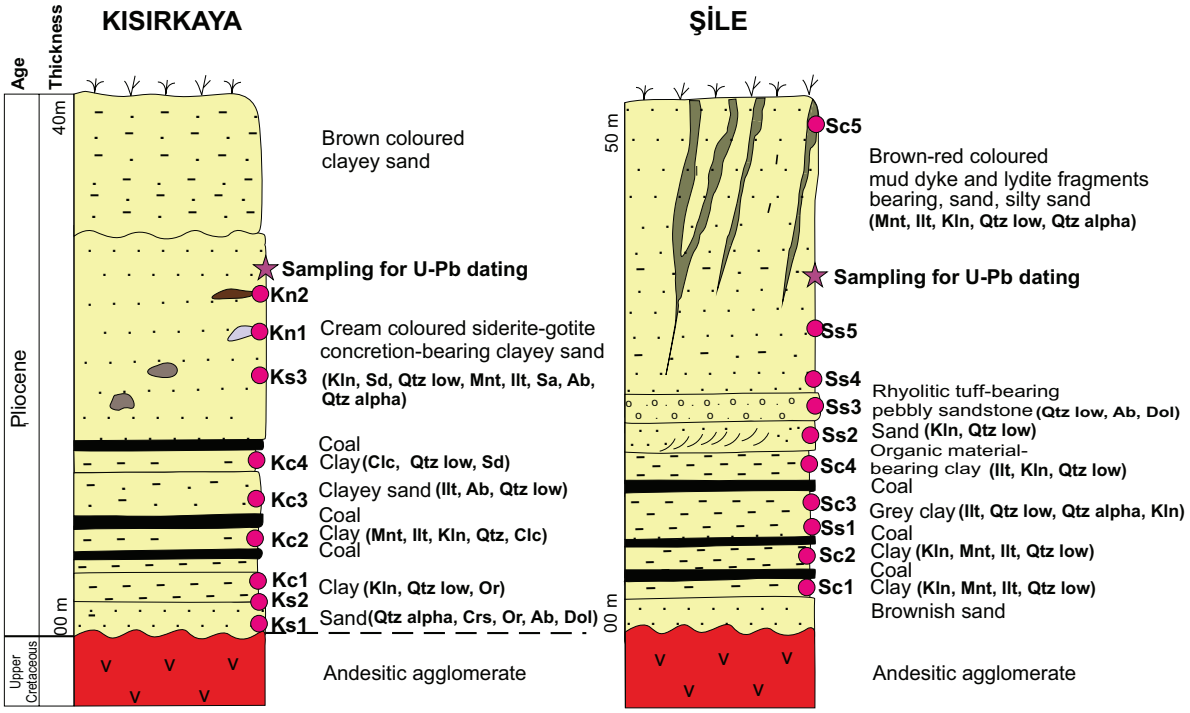

Fig. 2. Stratigraphic column section for Pliocene clay–sand–coal deposits in the Şile region (**a**) and the Kısırkaya region (**b**). The sections show the sampling horizons for geochemical and mineralogical analyses. Abbreviations: kln=kaolinite, ilt=illite, mnt=montmorillonite, qtz=quartz, sd=siderite, ab=albite, or=orthoclase, sa=sanidine.

the Kısırkaya sand is also relatively coarse-grained and includes abundant muscovite flakes and siderite concretions. Diagenetically formed elliptical and spherical siderite concretions with light brown colour occur at dimensions of a few centimetres to several metres in the sand (Fig. 3d). The uppermost fine-grained sand and silt levels of the Pliocene in the Kısırkaya region are eroded; for this reason, mud dykes are similar to the Şile region (Fig. 3c) cannot be seen here.

Although there are many studies about the geology of İstanbul, the age of these sand–clay–coal alternating deltaic sediments could not be determined clearly. Like most researchers (Yılmaz et al. 2000; Siyako 2006; Özgül et al. 2011; Şengör 2011), we accept its age as Pliocene. However, we have not observed contact relationships with Miocene formations, generally known as the Çekmece formation (Özgül et al. 2011).

Analytical methods and sample descriptions

Analytical methods

Samples were analysed for their mineralogical compositions by XRD. These analyses were carried out on powdered samples using a GNR APD-2000 Pro diffractometer in the X-ray diffraction laboratory of İstanbul University – Cerrahpasa, Department of Geological Engineering. Diffraction data were acquired by exposing the powdered samples to Cu-K_α X-ray radiation, which has a characteristic wavelength (λ) of 1.5418 Å. X-rays were generated from a copper (Cu) anode supplied with a voltage of 40 kV and a current of 30 mA. A goniometer speed of 2θ=1°/min was set during the analyses. The data were collected over a range of 5° to 55° for 2θ values, step size of 0.02°, divergence slit=0.5 mm and receiving slit=0.3 mm. Analysis of the X-ray patterns (phase identification) was carried out by using Philips High Score Plus software in conjunction with the JCPDS (Joint Committee on Powder Diffraction Standards) database.

Whole-rock chemical compositions of the studied samples were conducted at the Geochronology and Geochemistry laboratory of İstanbul University – Cerrahpasa (IUC-GGL), Department of Geological Engineering using a Perkin Elmer Avio 200 ICP-OES system. This package includes all major oxide (SiO_2, TiO_2, Al_2O_3, Fe_2O_3, MnO, MgO, CaO, K_2O, Na_2O, and P_2O_5) analyses after $LiBO_2$ fusion. The loss on ignition is given as the weight difference after ignition at 1050 °C. Trace and rare-earth element concentrations were examined using a Perkin Elmer NexION 2000 mass spectrometer and ESI NWR-213 solid-state laser ablation system established at the IUC-GGL, Turkey. The crater size was chosen as 110 microns for the analyses, the energy level was 7 joules, the repetition rate was 10 Hz, and NIST SRM610, SRM612, BCR2G, and AGV2G were the primary reference materials. During the measurements, 30 seconds gas blank, 30 seconds ablation time, and 50 seconds washout were selected. He (0.7 l/sec) was used as the carrier gas. Data reduction was performed using the SILLS software package (Guillong et al. 2008).

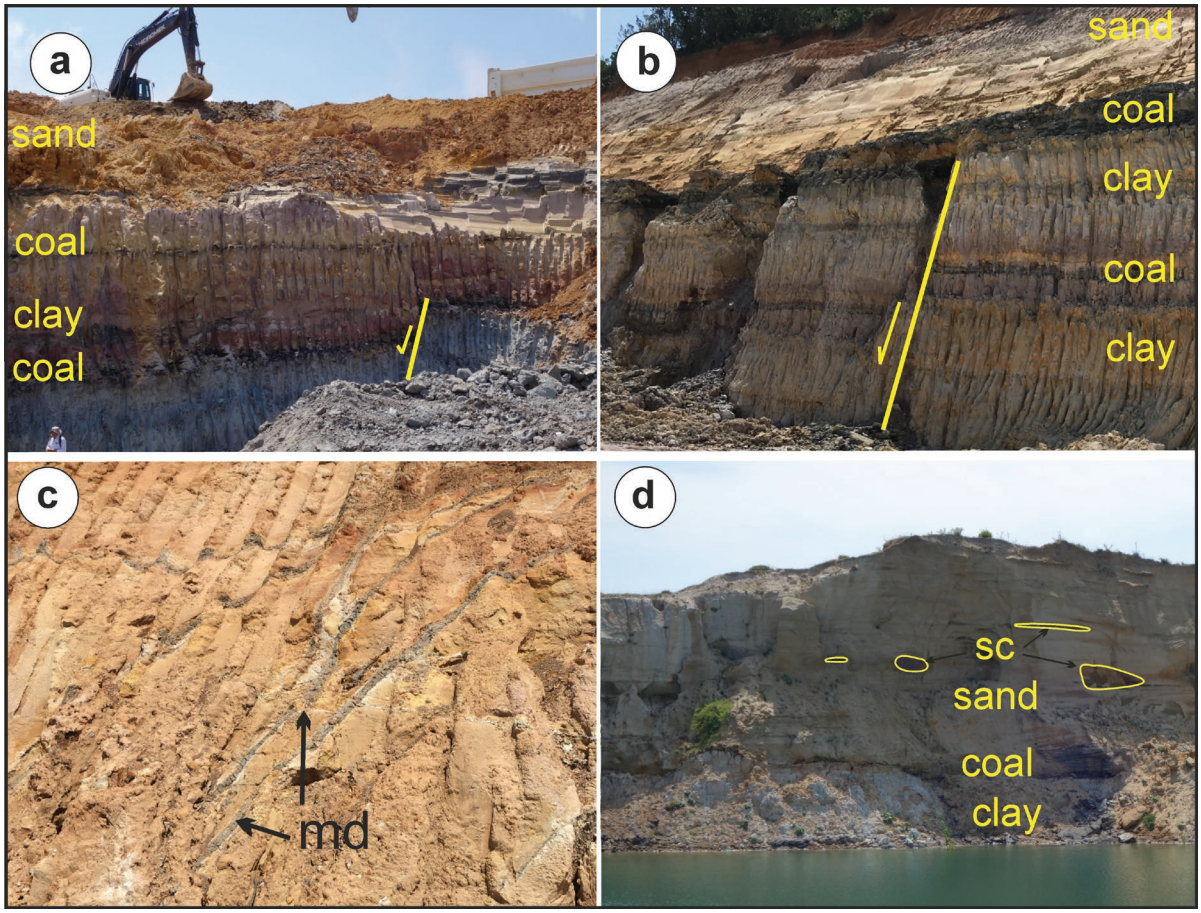

Fig. 3. Field photographs of Pliocene deposits in Şile (**a–c**) and Kısırkaya (**d**) regions. **a, b** — Syn-sedimentary normal faults with E–W strike and north dip in the Pliocene, showing metre-scale displacements related to subsidence of the sedimentary basin matter; **c** — Mud dykes with vertical and 45-degree angles common in silty sands located at the top of the Pliocene sequence; **d** — Coal, clay, sand levels at Kısırkaya quarry where clay and coal alternate levels are located under the upper sands. Lenticular, light brown coloured siderite concretions are a few cm to a few meters in size in sands. Abbreviations: md=mud dyke, sc=siderite concretion.

The zircon grains from the sand samples were separated by using traditional magnetic separation heavy liquid techniques after crushing, grinding, sieving and cleaning processes. Hand-picked zircon grains were mounted in an epoxy resin under a binocular microscope, and polished. U–Pb isotope analyses were carried out using a New Wave Research Excimer 193 nm laser-ablation system (NWR UP-193FX) attached to a Perkin-Elmer ELAN DRC-e inductively coupled plasma mass spectrometer (LA-ICP-MS) at the Geological Institute, Bulgarian Academy of Science in Sofia, Bulgaria. Laser crater size of 30 microns was selected in the analysis, and 0.5 l/s Helium was used as carrier gas. GEMOC GJ-1 (~608 Ma) was used as the primary standard reference material, and Plesovice (~337 Ma) was used as the secondary standard reference material. Raw data were processed using GLITTER, a data reduction program of the GEMOC, Macquarie University, Australia (http://www.gemoc.mq.edu.au/). Different types of zircon grains and their zones (cores and rims) were identified on CL images before analysis. Zircons are generally transparent, colourless, brownish, yellow, and rarely purple in colour. Most of the zircon grains are sub-idiomorphic, and idiomorphic, and some of them have well-rounded shapes. The internal structures of zircons are variable, and most of them consist of typical magmatic oscillatory zoning. Considering zircon morphology, some zircon grains are affected by long-term weathering and/or transport processes. For the classification of zircon populations, $^{206}Pb/^{238}U$ ages were used for zircons younger than 1 Ga, and $^{206}Pb/^{207}Pb$ ages were used for ones older than 1 Ga. Concordia diagrams and probability density plots were prepared using the Isoplotr (Vermesch 2018). Analytical error ranges in diagrams are generally given at the 1-sigma level. The geological time scale (Walker et al. 2018) was used as a stratigraphic reference for data interpretation.

Sampling and sample description

The samples used for geochemical and mineralogical analyses were obtained from the open-pit mine of Gözde Eren mining company in the Şile region and an abandoned open pit quarry in the Kısırkaya region. The sandy sediments are weakly cemented in both locations. Sand sampling to obtain zircon was performed from the uppermost clastics, whereas

clay sampling was made at the bottom part of the clastics. Light brown concretions were collected from a sandy level of the sedimentary succession in Kısırkaya. The sampling locations, coordinates, lithology, and other sedimentary features are summarized in Table 1.

Whole-rock geochemistry

Major oxides

The geochemical analysis results for samples obtained from the Şile and Kısırkaya sections are given in Table 2. According to the results obtained from XRD analyses, the mineral compositions of sands from the Şile and Kısırkaya regions are dominated by quartz and clays, which is consistent with chemical composition.

The SiO_2 contents of sand and clay samples vary in a wide range (31.78–95.79 wt.%) depending on the clay content. Al_2O_3 contents are between 1.97 and 28.56 wt.%, TiO_2 contents 0.05–2.72 wt.%, and Fe_2O_3 contents 0.27 to 47.40 wt.% reflect this change. The contents of MgO (0.03–1.16 wt.%), CaO (0.01–2.41 wt.%), Na_2O (0.03–2.23 wt.%), and K_2O (0.12–3.69 wt.%) are generally lower than the other oxides. Low amounts of alkali and alkali earth elements indicate strong leaching and removal of these elements during diagenesis in acidic conditions.

Trace elements

Trace elements reveal preferential enrichment in the clay layers relative to sands. Sc, V, Co, Ni, Cu, Zn, Pb, Ga, Se, Y, Sn, Sb, Cs, REEs, Bi, Nb, Zr, Th, Ta, and U have higher values in clays compared to sands (Table 3). Therefore, the Pliocene sediments in the Şile region contain a higher amount of trace elements, since they consist of finer-grained sediments compared to the Kısırkaya region (Fig. 4).

High field strength elements (HFSE), Zr, Ti, Nb, Hf, and Y prefer Si-rich felsic rocks during crystal fractionation and/or anatexis processes (Feng & Kerrich 1990), and values were higher than the upper continental crust (UCC) (Fig. 4a, b). Similarly, the average Zr/Hf ratios in these samples vary between 28.72 and 45.87 (average 38.34), which are relatively higher than the upper continental crust (UCC) values (32.76, McLennan 2001), and this is likely to indicate a felsic source. Th/U contents of the Şile and Kısırkaya samples are between 1.59 and 5.48 (mean 2.86), and these values are generally lower than the average upper crust value (UCC mean 3.82). A very distinctive Sr depletion in sand and clay relative to the continental crust is quite striking on the spider diagram

Table 1: Sample descriptions.

Location	Geographic Coordinates	Lithology	Sampling Method
Şile, İstanbul	41°8'44.09"N, 29°27'38.77"E	Weakly cemented fine-grained sand, clay	Outcrop samples from open pit quarry, fine-grained sand (50 kilos) for zircon separation
Kısırkaya, İstanbul	41°14'58.94"N, 28°58'20.34"E	Weakly cemented sand, clay	Outcrop samples from open pit quarry, fine-grained sand (50 kilos) for zircon separation

Table 2: Major oxide compositions of the sands and clays from Sile and Kısırkaya Pliocene sequences (SS=Şile sand, SC=Şile clay; KS=Kısırkaya sand, KC=Kısırkaya clay, KN=Kısırkaya concretion, b.d.l.=below dedection limit).

Sample	SiO_2	TiO_2	Al_2O_3	Fe_2O_3	MnO	MgO	CaO	Na_2O	K_2O	P_2O_5	LOI	SUM
SS 5	82.38	0.05	4.30	0.26	0.00	0.03	b.d.l	0.04	0.12	0.03	13.26	100.48
SS 4	73.12	2.72	11.80	4.08	0.07	0.20	0.01	0.03	0.46	0.09	7.38	99.96
SS 3	84.83	0.36	6.11	0.27	0.00	0.07	b.d.l	0.03	0.31	0.04	8.21	100.23
SS 2	92.53	1.19	3.94	0.33	0.01	0.05	0.01	0.03	0.36	0.07	1.97	100.50
SS 1	92.53	0.27	4.43	0.63	0.00	0.17	b.d.l	0.06	1.16	0.04	1.40	100.70
SC 5	50.15	0.96	25.65	9.99	0.01	0.88	0.03	0.09	1.21	0.02	10.87	99.86
SC 4	59.05	1.52	24.91	2.16	0.01	1.16	0.10	0.12	3.69	0.06	7.19	99.96
SC 3	54.53	1.46	19.64	10.60	0.12	0.99	0.14	0.09	3.12	0.05	9.24	99.99
SC 2	43.94	0.85	28.56	3.16	0.00	1.00	0.03	0.13	2.41	0.06	20.66	100.80
SC 1	65.62	0.87	20.42	2.06	0.04	0.90	0.09	0.07	2.34	0.10	7.31	99.83
KN 2	31.78	0.66	5.51	39.23	0.22	0.24	0.04	0.14	0.85	0.09	22.56	101.31
KN 1	32.65	0.95	9.50	33.44	0.17	0.58	2.41	0.16	1.22	1.27	16.89	99.22
KC 4	31.79	0.57	4.71	47.40	0.44	0.41	0.04	0.10	0.72	0.03	14.65	100.86
KC 3	66.94	0.31	9.99	1.52	0.02	0.64	1.58	2.23	2.05	0.09	15.30	100.68
KC 2	59.04	2.58	21.34	1.87	0.01	0.65	0.12	0.26	1.38	0.07	12.46	99.77
KC 1	69.50	1.39	17.05	1.77	0.00	0.64	0.38	0.35	1.73	0.06	7.41	100.27
KS 3	73.63	0.48	7.47	2.90	0.03	0.69	0.75	1.61	1.75	0.10	10.48	99.88
KS 2	95.79	0.33	1.97	0.40	0.01	0.09	0.09	0.48	0.84	0.05	0.45	100.50
KS 1	90.42	0.43	4.91	0.98	0.02	0.25	0.43	0.81	1.11	0.05	1.52	100.92

Table 3: Trace element compositions (ppm) of the clays, sands and concretions from Şile and Kısırkaya Pliocene sequences.

Sample	Sc	V	Cr	Co	Ni	Ga	Ge	Rb	Sr	Y	Zr
SS 5	3.68	30.03	16.75	0.65	5.52	3.02	0	5.65	8.89	5.11	43.55
SS 4	11.38	126.4	3649.43	9.01	32.61	7.84	2.73	8.28	15.56	33.25	4583.83
SS 3	4.73	48.73	110.64	1.33	15.2	5.86	2.08	6.35	11.77	4.47	166.39
SS 2	7.27	62.47	593.25	1.64	14.59	5.84	1.2	3.7	23.16	18.92	816.66
SS 1	5.68	61.63	21.95	2.5	15.97	6.47	0.64	35.44	13.88	11.89	100.83
SC 5	19.38	217.21	207.98	8.33	69.18	26.34	2.29	78.78	35.65	15.57	178.91
SC 4	16.24	156.86	57.59	5.44	33.07	24	1.3	173.04	35.82	24.36	211.89
SC 3	12.7	149.14	66.84	15.69	44.86	21.36	2.04	156.79	25.62	36.08	195.69
SC 2	21.69	156.81	95.27	11.29	49.17	27.18	2.23	114.01	54.49	16.6	157.74
SC 1	17.36	124.55	39.55	9.62	9.18	23.77	3.45	97.43	22.85	61.34	194.03
KN 2	12.46	125.77	51.34	15.58	16.18	7.48	0.85	33.88	25.58	17.48	135.58
KN 1	15.15	154.57	77.4	11.77	25.92	11.22	1.14	51.05	89.44	19.94	150.68
KC 4	11.8	102.5	56.18	25.91	40.96	8.83	0.98	32.03	33.47	33.43	133.52
KC 3	7.03	57.51	164.53	6.79	53.16	7.84	1.15	54.23	285.95	10.09	85.98
KC 2	16.83	140.84	81.13	18.82	49.28	21.53	0	62.48	68.7	23.48	256.91
KC 1	14.59	142.51	107	6.32	59.05	16.66	2.26	82.99	37.25	14.04	233.68
KS 3	6.98	66.86	459.82	7.2	57.6	7.11	1.52	41.37	129.94	13.69	222.29
KS 2	3.77	46.02	534.73	1.3	13.1	2.79	0.3	17.97	33.03	5.94	164.39
KS 1	6.66	63.3	342.04	4.43	29.19	5.95	0	30.78	62.81	6.23	72.98

Sample	Nb	Cs	Ba	Hf	Ta	W	Tl	Pb	Th	U
SS 5	1.29	0.35	27.48	1.06	0.11	0.14	0.07	5.08	1.43	0.349
SS 4	25.82	0.55	54.52	112.05	2.52	2.14	0.08	14.44	37.45	10.648
SS 3	4.79	0.56	23.74	4.18	0.41	0.79	0.2	15.3	4.49	0.82
SS 2	20.3	0.24	31.79	18.58	1.61	2.51	0.07	13.74	8.81	3.608
SS 1	5.96	1.46	120.81	2.25	0.57	0.74	0.18	26.41	4.46	2.263
SC 5	15.49	7.31	151.26	4.58	1.33	2	0.27	23.22	17.02	3.418
SC 4	19.62	8.21	552.26	5.49	1.76	3.12	0.84	28.38	9.58	3.897
SC 3	20.44	8.16	431.88	5.37	1.77	4.18	0.73	52	14.14	7.648
SC 2	11.43	9.3	405.64	4.5	1.18	1.56	0.5	15.59	11.66	3.408
SC 1	11.33	7.54	114.84	4.92	0.72	1.85	0.75	57.99	9.49	4.015
KN 2	7.69	2.09	190.01	3.65	0.65	0.64	0.18	4.57	3.85	1.647
KN 1	10.08	3.13	310.29	4.36	0.72	1.09	0.26	10.47	5.97	3.018
KC 4	7.19	1.6	173.52	3.81	0.63	0.92	0.31	5.77	2.89	1.088
KC 3	3.44	1.21	552.62	2.5	0.4	0.33	0.43	10.3	4.39	0.984
KC 2	26.64	8.44	261.98	7.65	2.42	3.52	0.31	14.82	9.54	4.742
KC 1	16.61	4.61	246.43	5.75	0.97	1.88	0.4	7.18	4	2.515
KS 3	5.54	1.82	259.21	4.85	0.26	0.6	0.13	7.38	4.64	1.792
KS 2	4.85	0.51	96.75	4.16	0.42	0.91	0.37	5.42	2.03	0.89
KS 1	7.21	1.09	164.37	2.54	0.33	0.97	0.34	7.81	3.06	1.643

(Fig. 4a, b). In the chondrite-normalized REE diagrams (Sun & McDonough 1989), a distinct negative Eu anomaly is also typical and indicates Sr^{2+} and Eu^{+2}, which have similar ionic radii, were completely dissolved from feldspars in the weathering environment and transported from the drainage basin into the sea.

Rare earth elements

REE concentrations of the Şile and Kısırkaya samples are given in Table 4, and chondrite-normalized spider diagrams are given in Figure 4. The total REE (ΣREE) contents of the Şile and Kısırkaya samples are between 20.81 and 892.32, with an average of 148.26 ppm. The lowest ΣREE value (20.81) was obtained from a sand sample with a SiO_2 content of 82.38 wt.% and the highest ΣREE value (892.32 ppm) was found in a clay sample with a SiO_2 content of 65.62 wt.%. The average value is close to the average upper crust value (146.37 ppm). The Eu/Eu* ($=(Eu/Eu_{CN})/[\sqrt{(Sm/Sm_{CN})}\times(Gd/Gd_{CN})]$) values are between 0.39–1.12 (avg. 0.80) for the Şile and Kısırkaya samples. The Eu/Eu* value varies significantly between mafic and felsic source rocks and is, therefore, an important argument for distinguishing mafic and felsic source contributions in sedimentary rocks. All Eu/Eu* values are below 1, except for two samples, and exhibit negative Eu anomaly (Fig. 4c, d). Chondrite-normalized negative Eu anomaly indicates a provenance containing acidic magmatic or aluminosilicate rocks of metamorphic massifs.

Detrital zircon U–Pb ages

Many detrital-geochronology techniques (e.g., zircon, rutile, and garnet U–Pb dating) are common methods used to identify the origin of clastic sediments and to reconstruct

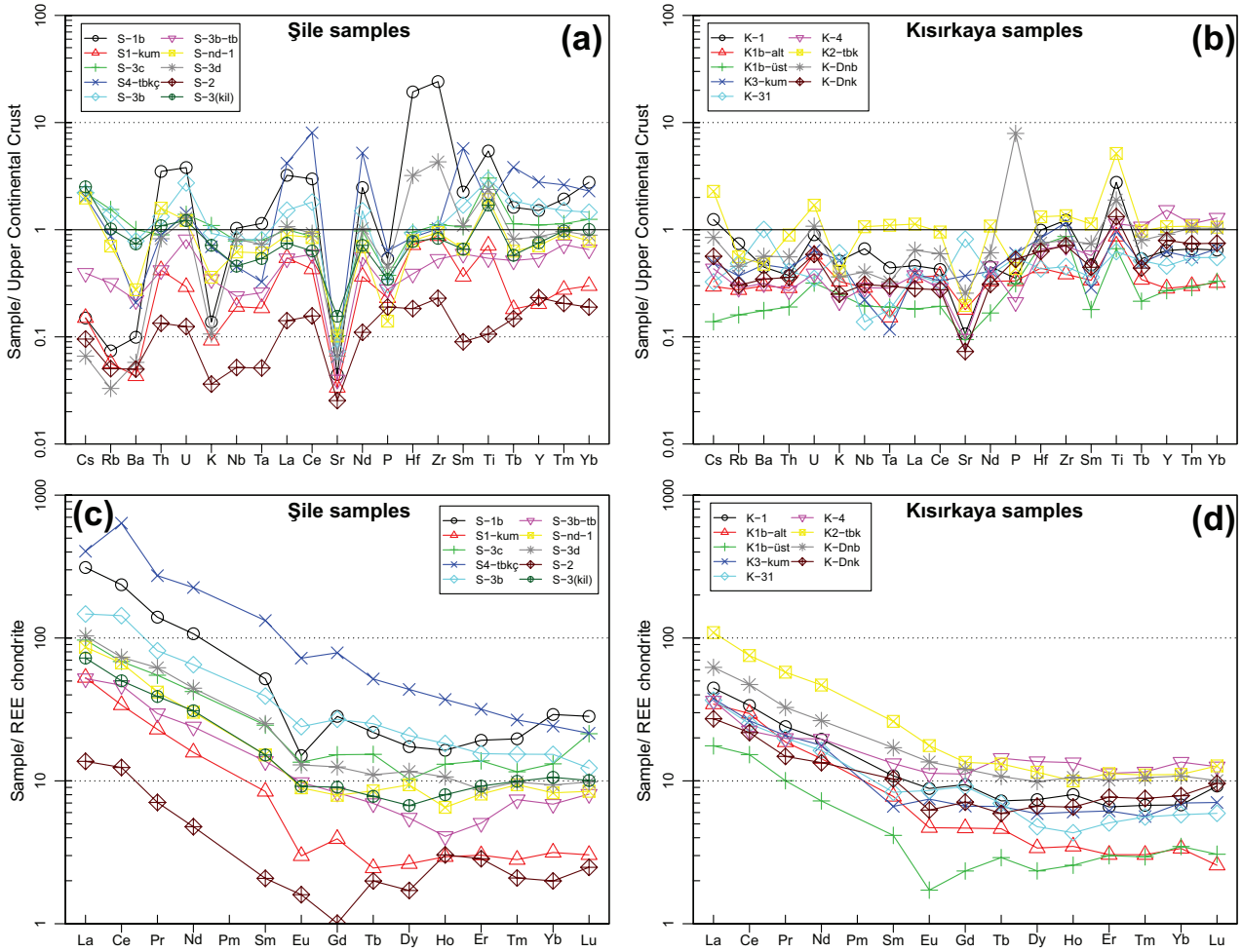

Fig. 4. a, b — Upper continental crust (Taylor & McLennan 1989) – normalized trace elements, and **c, d** — Chondrite-normalized REE diagrams (Sun & MacDonough 1998) for the Şile and Kısırkaya sands and clays.

palaeogeography. For the source region analyses of the İstanbul Pliocene sequence, detrital zircon U–Pb ages were obtained from sand samples taken from Şile in the east and Kısırkaya in the west of the Bosphorus. A total of one hundred and five points were dated on one hundred selected zircon grains (Fig. 5) from the Şile sands, and 90–110 % concordant ages were obtained for eighty-four points (Supplementary Table S1, Fig. 6). The youngest 22.98±0.95 Ma and the oldest 2292±38 Ma $^{206}Pb/^{238}U$ were obtained from the Şile sands. The youngest 53±2 Ma ($^{206}Pb/^{238}U$, 93 % concordant, Th/U=0.35) and the oldest 2396.9±72 ($^{206}Pb/^{207}Pb$, 97.1 % concordant, Th/U=0.48) were obtained from eighty-seven points concordant between 90–110 %. Nine points in the 22.18±0.95–63±1.8 Ma age interval (8.57 % Tertiary), ten points in the 71.8±1.2–248.8±4.4 Ma age interval (9.52 % Mesozoic), seventy-five points in the 259.3±4–540±12 Ma Ma age interval (71.43 % Paleozoic), seven points in the 550.6±8.2–793±21 Ma age interval (6.67 % Neoproterozoic), and four points in 1580±130–2396±72 Ma age interval (3.81 % Mesoproterozoic–Paleoproterozoic) were measured on one hundred zircon grains (Fig. 6). Therefore, it can be concluded that 71.43 % of zircon populations are concentrated in the Paleozoic period. Five of the seven ages belonging to the Neoproterozoic period are in the age range of 550.6±8.2 –632±20 Ma (Ediacaran). The distribution of seventy-five Paleozoic ages is as follows: six in the 504±13–540±12 Ma age interval (8 % Cambrian), ten points in the 447±11–479±16 Ma age interval (13 % Ordovician), seven points in the 422.5±9.8–441±11 Ma age interval (9 % Silurian), fifteen points in the 366±11–417±10 Ma age interval (20 % Devonian), twenty-seven points in the 299.7±5.2–357.4±9.3 Ma age interval (36 % Carboniferous), and ten points in the 259.3±4–298±5.2 Ma age interval (13 % Permian). The distribution of nineteen measured points that give Mesozoic–Tertiary ages are as follows: three in the 220±11–248.8±4.4 Ma age interval (Triassic), seven points in the 71.8±1.2–132.7 ±4.8 Ma age interval (Cretaceous), seven points in the 50±2.3 –63±1.9 Ma age interval (Paleocene–Eocene), and seven points in the 22.18±0.95–23.23±0.97 Ma age interval (late Oligocene–early Miocene). The Th/U ratios of zircon grains are between 0.01 and 1.41 (Supplementary Table S1). Th/U ratios of metamorphic zircons are generally less than 0.1 in

Table 4: Rare earth element compositions (ppm) of the Şile and Kısırkaya Pliocene sediments.

Sample	La	Ce	Pr	Nd	Sm	Eu	Gd	Tb	Dy	Ho	Er	Tm	Yb	Lu
SS 5	4.25	10.03	0.86	2.86	0.41	0.12	0.26	0.09	0.55	0.22	0.60	0.07	0.42	0.08
SS 4	96.54	190.68	17.07	64.27	10.10	1.10	7.33	1.03	5.59	1.18	4.04	0.64	6.09	0.91
SS 3	16.37	27.45	2.80	9.50	1.64	0.22	1.02	0.12	0.85	0.21	0.63	0.09	0.66	0.10
SS 2	32.06	59.25	7.55	26.72	4.91	0.95	3.24	0.52	3.75	0.76	1.83	0.32	1.96	0.32
SS 1	16.13	37.71	3.61	14.34	2.68	0.72	2.14	0.33	1.77	0.29	1.06	0.24	1.44	0.26
SC 5	26.75	54.00	5.10	18.13	2.96	0.66	2.05	0.40	3.02	0.47	1.70	0.30	1.72	0.27
SC 4	30.00	55.33	6.70	25.32	4.79	0.99	3.95	0.73	3.29	0.94	2.90	0.38	2.75	0.69
SC 3	45.64	115.82	9.93	39.04	7.65	1.76	6.99	1.19	6.68	1.31	3.26	0.50	3.20	0.40
SC 2	22.44	40.54	4.75	18.58	2.96	0.67	2.34	0.37	2.16	0.57	1.93	0.32	2.21	0.32
SC 1	125.41	514.19	33.33	135.37	25.85	5.31	20.41	2.45	14.06	2.67	6.66	0.86	5.05	0.69
KN 2	8.44	17.61	1.81	8.05	2.01	0.46	1.84	0.28	2.14	0.47	1.61	0.24	1.65	0.31
KN 1	19.31	38.18	3.98	15.85	3.33	1.00	3.13	0.51	3.18	0.76	2.13	0.34	2.26	0.32
KC 4	11.26	18.12	2.42	11.78	2.58	0.83	2.89	0.68	4.40	0.96	2.37	0.37	2.83	0.40
KC 3	11.38	20.29	2.43	9.81	1.62	0.63	2.37	0.33	1.54	0.31	1.07	0.18	1.21	0.19
KC 2	33.84	60.93	7.03	28.11	5.09	1.30	3.49	0.62	3.71	0.72	2.36	0.36	2.32	0.41
KC 1	13.85	27.22	2.93	11.73	2.11	0.65	2.44	0.34	2.38	0.58	1.38	0.22	1.42	0.30
KS 3	11.66	21.30	2.54	10.64	1.29	0.55	1.72	0.31	1.90	0.43	1.29	0.18	1.46	0.23
KS 2	5.45	12.33	1.22	4.34	0.81	0.13	0.61	0.14	0.75	0.18	0.63	0.10	0.73	0.10
KS 1	10.68	23.91	2.28	8.58	1.52	0.35	1.21	0.22	1.09	0.25	0.64	0.10	0.70	0.08

twenty-six grains. Th/U ratios of 0.1–1.41 in seventy-nine grains indicate that zircons have felsic magmatic and mafic-felsic transition origin (Teipel et al. 2004; Linnemann et al. 2011).

A total of one hundred measurements were done on ninety-six zircon grains (Fig. 5) separated from the Kısırkaya sands, and seventy-three of them had 90–110 % concordant ages (Supplementary Table S2; Fig. 7). The youngest 23.93±0.77 Ma and the oldest 2020±12Ma $^{206}Pb/^{238}U$ were taken from one hundred data points from the Kısırkaya sands. The youngest 24.5±1 Ma ($^{206}Pb/^{238}U$, 103.4 % concordant, Th/U=0.23) and the oldest 2057±22 Ma ($^{206}Pb/^{207}Pb$, 99.61 % concordant, Th/U=0.58) were taken from seventy-seven points concordant between 90–110 %.

Zircon grains had twenty-seven points measured in the 23.93±0.77–59.1±1.7 Ma age interval (27 % Tertiary), fifteen points in the 72.9±1.3–215.3±4.5 Ma age interval (15 % Mesozoic), thirty-eight points in the 258.9±5.2–494.8±5.1 Ma Lineman age interval (38 % Paleozoic), sixteen points in the 542.4±7.9–999±11 Ma age interval (16 % Neoproterozoic), and four points in 1834±61–2057±22 Ma age interval (4 % Mesoproterozoic–Paleoproterozoic). While 38 % of the zircon populations were concentrated in the Paleozoic period, 27 % of the zircons were concentrated in the Tertiary period. Seven of the Neoproterozoic zircons were concentrated in the Ediacaran period with an age range of 542.4±7.9–620±11 Ma, while one point represents Cryogenian and two points represent the Tonian period. The distribution of thirty-eight points that give Paleozoic age is as follows: two in the 504±13–540±12 Ma age intervals (3 % Cambrian), thirteen points in the 443.8±4.9–484±12 Ma age interval (13 % Ordovician), four points in the 427±13–442.5±6.2 Ma age interval (4 % Silurian), one point at 365.9±7.2 Ma age (1 % Devonian), nine points in the 305.1±8.7–348.7±5.6 Ma age interval (9 % Carboniferous), and nine points in the 258.9±5.2–297.9±3.9 Ma age interval (9 % Permian).

The distribution of forty-four points that give Mesozoic–Tertiary ages are as follows: one at 215.3±4.5 Ma age (Triassic), four points in the 155.7±4–161.6±2 Ma age interval (Jurassic), twelve points in the 72.9±1.3–98.2±4.4 Ma age interval (Cretaceous), nineteen points in the 34.39±0.8–59.1 ±1.7 Ma age interval (Paleocene–Eocene), and eight points in the 23.93±0.77–31.1±1.2 Ma age interval (Oligocene–Miocene). The Th/U ratios of zircon grains are between 0.01 and 1.85 (Supplementary Table S2). Th/U rates of metamorphic zircons are generally less than 0.1 in three grains. Th/U ratios of 0.1–1.85 in ninety-seven grains indicate that zircon grains have a felsic magmatic, mafic-felsic transition, and mafic magmatic origin.

Discussion

The depositional environment of the İstanbul Pliocene

İstanbul Pliocene deposits unconformably overlies Upper Cretaceous volcaniclastics. This contact is observed at an altitude of about 80 meters in the Şile region and 15 meters in the Kısırkaya region, and this can be explained as due to the Kısırkaya Pliocene sequence being downthrown by normal faults. In the Şile and Kısırkaya regions, the sedimentary series of clay–sand–coal alternation characterizes a delta environment and presents features similar to the Georgian kaolin deposits that occurred in the late Cretaceous in the USA (Walter et al. 1965; Pruett 2016). The Pliocene deposits were deposited at the mouth of a large river discharging into the Black Sea before the Sea of Marmara developed. The coal seam-bearing sedimentary sequence may have formed in the marshy area of a delta environment.

The fact that coal-lignite in the Pliocene sequence contains leaves, branches and tree roots indicates that fragments of

Fig. 5. Zircon cathodoluminescent images for the Kısırkaya (**a**), and Şile (**b**) sands. Red circles represent the dating points.

terrestrial plants were transported with suspended clays and accumulated in the delta plain. Kaolinitic clays are located just below the dark grey organic matter-rich sediments and represent a low energy environment. Thick kaolinite deposition with km-scale lateral extension indicates very good sediment sorting in the delta environment. E–W tending and north dipping syn-sedimentary normal faults can be considered as due to sediment loading and subsidence via normal faults in the depositional environment. Very well-rounded gravel layers in the uppermost levels indicate some short-term flooding and sediment fluxes into the deltaic ponds. The absence of fragments of İstanbul Paleozoic rocks such as limestone and quartzite among the coarse pebbles indicates that the fragments are also exogenic and come from distant areas.

There is no clear evidence about the age of this non-marine sedimentary sequence, which we call the İstanbul Pliocene. However, previous researchers mostly placed it above the upper Miocene sediments (Bakırköy Formation) represented by lagoon-brackish water deposits and assigned it a Pliocene age (Yılmaz et al. 2010; Şengör 2011). The Pliocene sediments must belong to the sedimentation period following Miocene lagoon filling, which entered the Marmara from the Black Sea in the west of İstanbul. Indeed, unconsolidated and undeformed deltaic sediments should be younger than those of the Çukurçeşme, Güngören and Bakırköy Formations belonging to the late Miocene. The İstanbul Pliocene can be correlated with the Ergene Formation which reaches a thickness of a few km in the Thrace Basin. However, the İstanbul

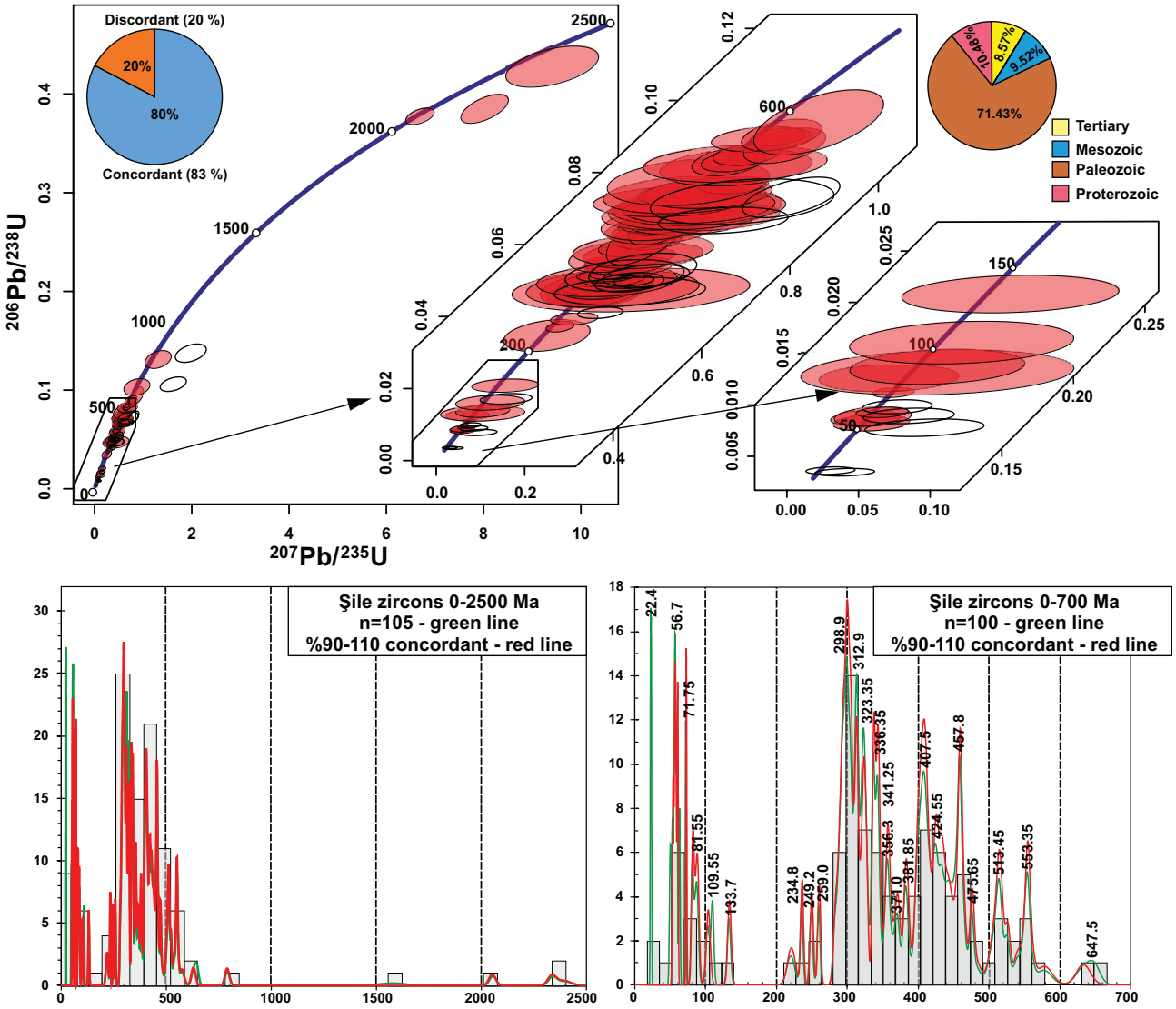

Fig. 6. Concordia diagram (upper) and probability density distributions (middle 0–2500 Ma and lower 0–700 Ma) for zircon ages obtained during this study from the Şile sands. $^{206}Pb/^{238}U$ was selected for ages <1000 Ma and $^{207}Pb/^{206}Pb$ for ages >1000 Ma in the diagram.

Pliocene sediments do not have contact with the Ergene Formation; thus, their stratigraphic relationship and relative age identifications cannot be clearly stated. The Pliocene formations are almost horizontally bedded on both sides of İstanbul, which indicates the presence of a peneplain and also a low topographic area at the Black Sea coast. The Pliocene river must have drained into the Black Sea, and the main axis of this river was probably the Bosphorus. Although there is post-Pliocene erosion, the presence of large Pliocene outcrops on both sides of İstanbul indicates that the İstanbul region was entirely covered by these deltaic sediments during that time. Therefore, the source of İstanbul's clay deposits cannot be Upper Cretaceous volcanites as stated by previous researchers (Ece et al. 2003) since the Upper Cretaceous volcanites underlie the Pliocene clastics on the coastal plain of the Black Sea (Fig. 1). It can be concluded that the İstanbul Pliocene deposits, which spread over much larger areas including today's Sea of Marmara depression, had higher sediment thickness than the İstanbul outcrops because sedimentation by Pliocene rivers continued in the Marmara depression after blockage by the İstanbul–Trakya horst.

Provenance and tectonic setting analysis with trace element geochemistry

The mineralogical composition and geochemical nature of siliciclastic sediments are used effectively to determine the source area for the basin where the sediments form and to predict palaeoclimatic conditions (Fedo et al. 1996; González-Álvarez & Kerrich 2012). There are many indices in the literature to evaluate the chemical change and climatic conditions depending on the chemical composition of the rock (Price & Velbel 2003; Depetris et al. 2014). The most widely used of these indexes is the chemical alteration index (CIA)

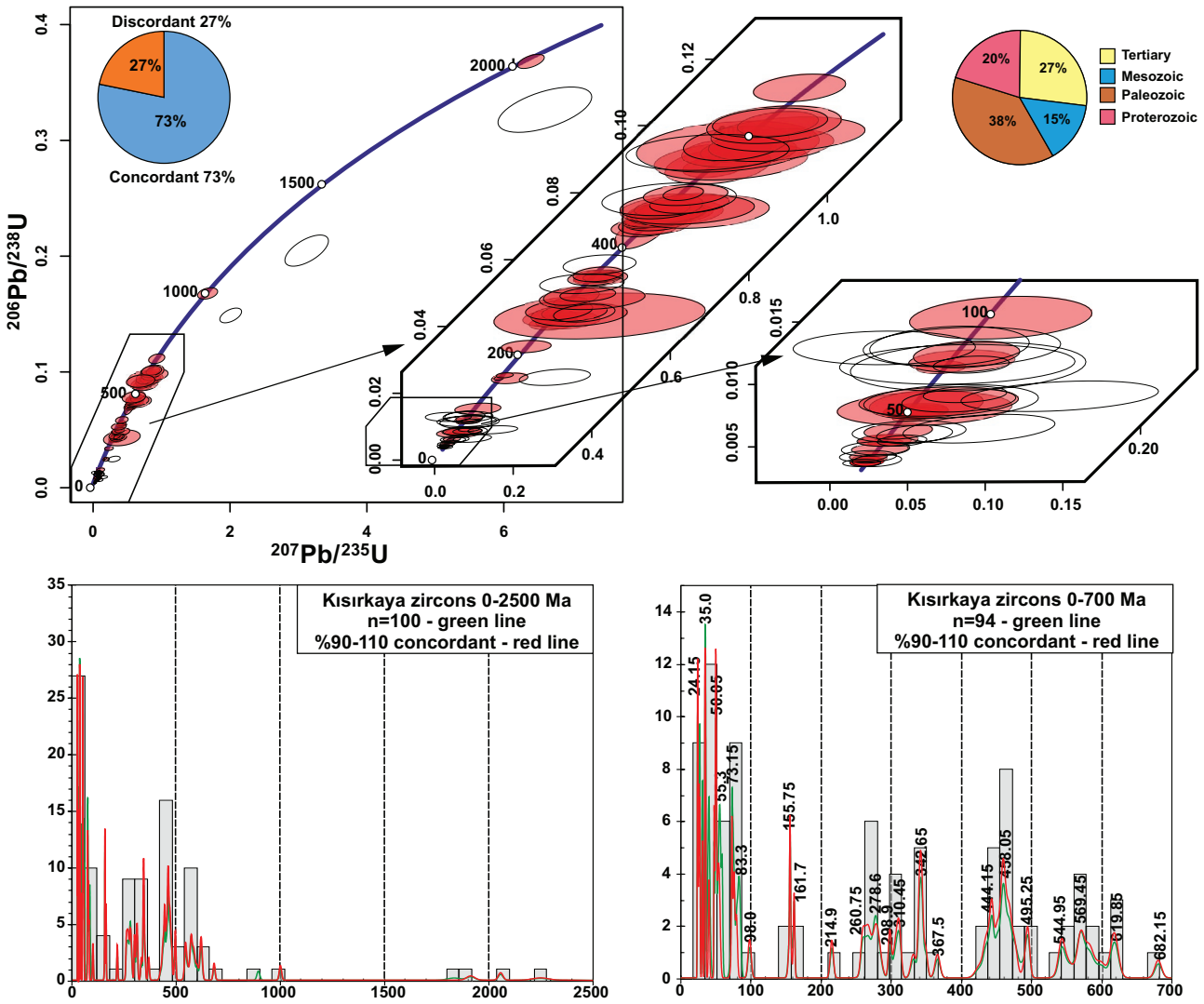

Fig. 7. Concordia diagram (upper) and probability density distributions (middle 0–2500 Ma and lower 0–700 Ma) for zircon ages obtained during this study from the Kısırkaya sands. $^{206}Pb/^{238}U$ was selected for ages <1000 Ma and $^{207}Pb/^{206}Pb$ for ages >1000 Ma in preparing the diagram.

proposed by Nesbitt & Young (1984). The chemical alteration index (CIA=$Al_2O_3/(Al_2O_3+CaO^*+Na_2O+K_2O)\times 100$; Nesbitt & Young 1984; the CaO* value represents the CaO content of the silicates) values for sedimentary rock samples taken from Şile and Kısırkaya vary between 53.14 and 96.94 (Table 2). Using the CIA values together with the A–CN–K (Al_2O_3–CaO^*+Na_2O–K_2O) triangular diagram of Nesbitt & Young (1984), observation of the weathering degree and mineralogical changes is possible. The samples taken from the Şile region show a weathering trend close to the kaolinite–gibbsite–chlorite–illite composition along the AK line on the A–CN–K triangular diagram (Fig. 8). This source indicates intense chemical weathering of rocks during supergene alteration and diagenesis. High CIA values indicate that samples from the Şile region contain higher clay minerals than feldspars, together with the fact that samples are far from the K-feldspar–plagioclase line and close to the kaolinite–gibbsite line.

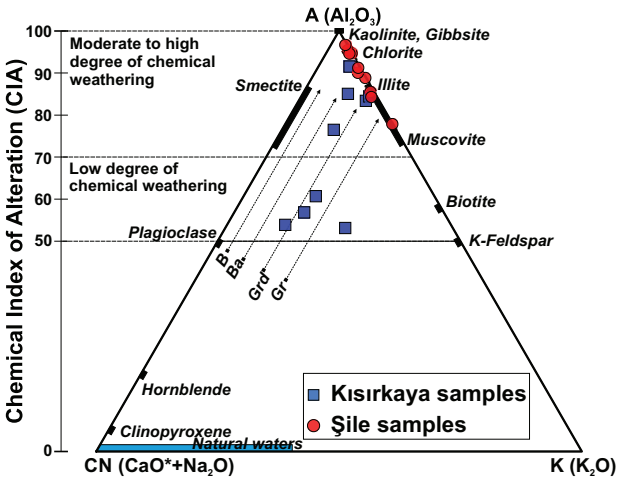

Fig. 8. A–CN–K diagram (Nesbitt & Young 1984) for the Şile and Kısırkaya Pliocene sediments.

Samples from the Kısırkaya region are different from the Şile region. Some of the samples show moderate weathering and are located close to the K-feldspar–plagioclase line. Similarly, all samples are arranged almost perpendicular to the A–K line and exhibit good coherence with the alteration tendencies of granitic, granodioritic, basaltic, and andesitic sources. Some of the samples are moderate to highly weathered and fall into the kaolinite, illite, smectite, chlorite, and muscovite fields. The K_2O/Na_2O ratio for the Şile and Kısırkaya samples was determined to be between 0.92–33.43 (mean 11.79), indicating that K-feldspar is more dominant than plagioclase in this source. On the other hand, high K_2O contents (up to 3.69 wt.%) indicate the presence of minerals rich in K such as mica. Plagioclase alteration index (PIA=$[(Al_2O_3-K_2O)/(Al_2O_3+CaO^*+Na_2O-K_2O)]\times 100$; Fedo et al. 1995) values range from 55.11 to 100. The depletion of CaO, NaO and Sr elements together with high PIA values indicates that the source rocks underwent moderate-severe chemical weathering, and plagioclase was weathered at the source.

Similarly, the still high Na_2O contents in the sand samples show that albite is partially preserved. The relatively high LOI values (15.30, 16.89) of two samples (1.58, 2.41) with high CaO content from the Kısırkaya sequence indicate probable carbonate contribution (calcite, dolomite and/or siderite). All these trends are also compatible with the mineralogical composition obtained from XRD analysis.

The Th/U ratios provide essential clues to determining the source characteristics of clastic sedimentary rocks (Roddaz et al. 2006). The average Th/U values for the Şile and Kısırkaya samples are 2.86, and except for a few samples, they are generally below the UCC (UCC: 3.82) values. However, Th/U ratios for the upper and lower mantle are 2.6 and 3.8 (Paul et al. 2003). Th scarcity relative to uranium in the sediments can be explained by the presence of ultrabasic rocks in the source area, or the precipitation of uranium during sedimentation or diagenesis. Rb, Sr, and Ba contents of the sediments have generally lower concentrations compared to UCC values, contrary to U (Fig. 4a, b), that correspond to intense removal of these elements owing to alteration at the source or in the depositional site. In some samples rich in K-feldspar and mica minerals, it is observed that Cs, Rb, Ba and K elements are increased compared to the upper crust values.

On the chondrite-normalized spider diagrams (Fig. 4c, d), clay and sand samples from both the Şile and Kısırkaya regions are enriched in light REE and heavy REEs. The high REE contents in the Şile and Kısırkaya samples are largely due to the presence of mica (mostly biotite and, to a lesser extent, muscovite) and feldspar minerals. Chondrite normalized REE patterns are similar to a felsic source.

Based on the whole-rock major oxide compositions, the samples from the Şile and Kısırkaya regions fall into the "quartz sedimentary source" field except for one "mafic igneous provenance" on the DF1 vs. DF2 source region diagram (Roser & Korsch 1988) (Fig. 9a). Although Cr is rich in the mantle and participates in the basic and ultrabasic rock formation, Th is a lithophile element and enriches the continental crust. Both elements are almost immobile under the surficial conditions and therefore, the Cr/Th value of the sediments gives valuable information about their source rocks and is widely used (McLennan et al. 1993; Cullers 1994, 2000). Similarly, Th/Sc and Th/Co values are similarly used in provenance analyses since Co and Sc are also specific to mantle rocks and are immobile under surface conditions.

The Th/Sc ratios are below the upper crust value, and they may have been derived from a source with andesitic composition. However, some of the Şile samples have Th/Sc ratios above the upper crust value, and Zr/Sc values are also high (Fig. 9b). This situation shows that some of the Şile samples matured by sediment reprocessing bringing zircon to the basin. The samples from Şile and Kısırkaya fall into the "mixed mafic–felsic source" field on the La/Th versus Hf diagram (Fig. 9c). The Cr/V versus Y/Ni diagram (Fig. 9d) also shows that the Kısırkaya samples were fed from both ultramafic source and felsic source, and the other samples mainly came from granitic source regions. Th and Cr are widely used as end elements in defining the source regions of rocks (Cullers 1994, 2000). Although Th is enriched in the continental crust, it is found with a very low concentration in the mantle.

Cr is enriched in ultramafic–mafic rocks and is extremely low in the continental crust. Therefore, the common feature of these two elements is that both are very difficult to dissolve and, therefore, immobile elements. The Th/Sc, Th/Cr, and Th/Co ratios given in Table 5 indicate that a significant number of clasts from an ultramafic–mafic source area was added to the Pliocene clay and sand deposits. Since there are no units that could be ultramafic sources in the east and west of İstanbul, it is thought that the mafic–ultramafic fragments in the Neogene sediments may have originated from ophiolitic rocks south of İstanbul. It is known that mafic–ultramafic rocks are common in the Intra Pontide zone south of the study area and further along the İzmir–Ankara–Erzincan suture zone in the S-SW direction. The presence of more ultramafic source field inputs in the Kısırkaya samples indicates that a significant amount of material was transported from the ophiolitic masses, especially along the south Marmara. Considering that the Marmara Sea had not yet opened during the Pliocene, a significant amount of Cr, Fe, and Ni-rich clastics were included in sediments discharged from the Intra-Pontide ophiolites and other ophiolitic belts further south into the Black Sea. Alpha quartz and cristobalite minerals forming at low temperatures in the mineralogical composition of the sands show that vein-filled quartz associated with hydrothermal alteration was transported in fluvial sediments together with clays.

Provenance analysis with zircon

The zircon ages obtained from the İstanbul Pliocene sequence provided important data about the possible age of the formation and interpretation of the source region. Zircon grains with different morphological features (well-rounded, semi-rounded, and euhedral), oscillatory zoning, and occasionally containing inherited cores were dated. Considering

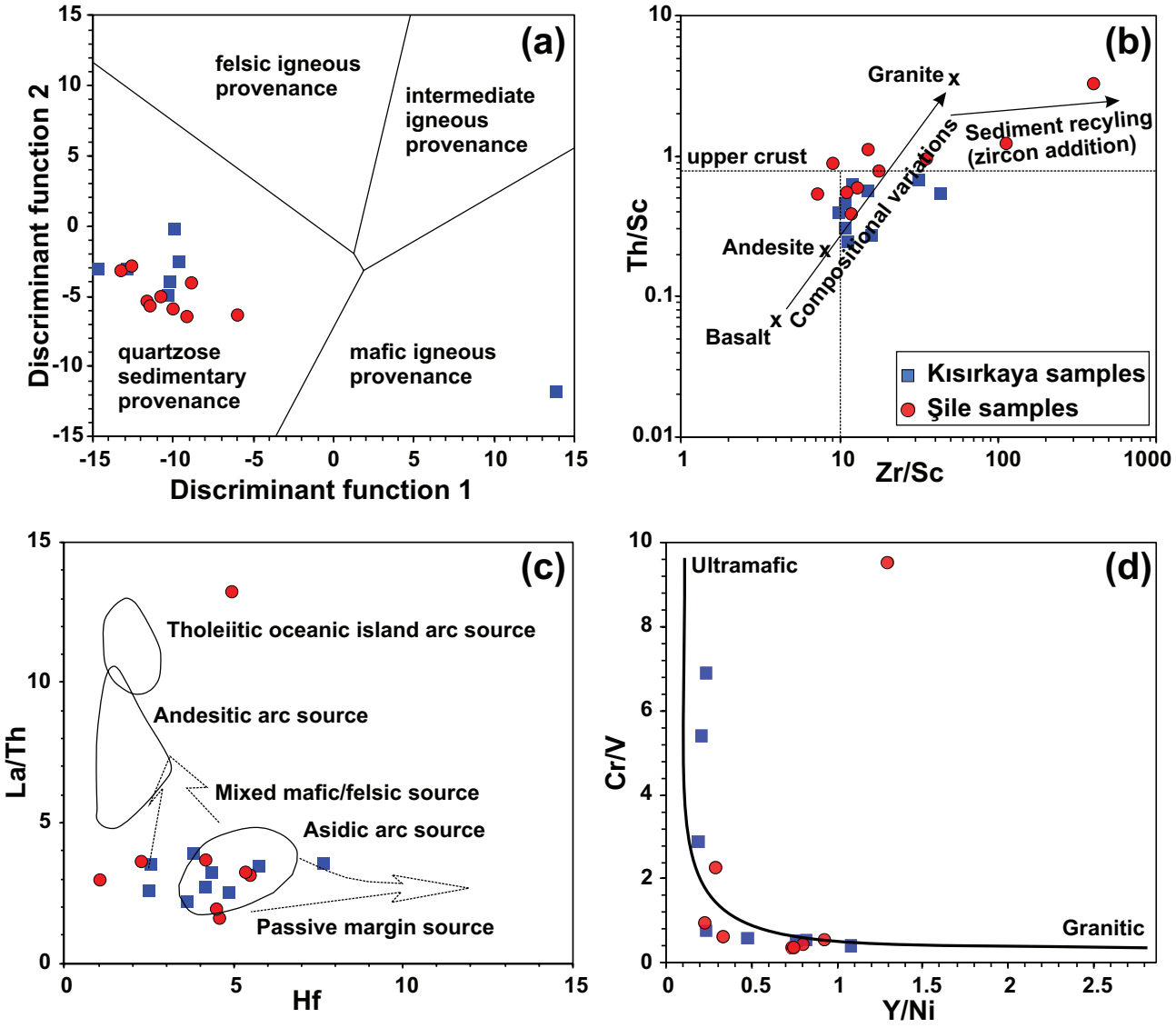

Fig. 9. a — Discriminant function diagram (Roser & Korsch 1988; Discriminant function 1=−1.773 TiO_2+0.76 Fe_2O_3t−1.5 MgO+0.616 CaO +0.509 Na_2O−1.224 K_2O−9.09; Discriminant function 2=0.445 TiO_2+0.07 Al_2O_3−0.25 Fe_2O_3t−1.142 MgO+0.438 CaO+1.475 Na_2O +1.426 K_2O−6.861); **b** — Th/Sc vs. Zr/Sc diagram (after McLennan et al. 1993); **c** — La/Th vs. Hf diagram (after Floyd & Leveridge 1987); and **d** — Cr/V vs Y/Ni diagram (after Mongelli et al. 2006) for the Şile and Kısırkaya samples.

the zircon shapes, some zircon grains are well-rounded and were subjected to long-term weathering-transport processes, while some were transported over short distances and have semi-rounded, or preserved prismatic crystal morphology. According to their internal structures, zircons are mostly magmatic zircons with oscillatory zoning, some of them have patchy internal structures containing inherited cores, and some have a cloudy appearance with weak and/or without zoning. Similarly, some zircons are surrounded by metamorphic halos. Mesoproterozoic–Paleoproterozoic ages were obtained at eight points in zircon grains collected from the Şile and Kısırkaya sands. $^{206}Pb/^{207}Pb$ ages from zircon grains vary between 1580±130 and 2396±72 Ma; there is no Mesoproterozoic–Paleoproterozoic magmatic activity described in the study area and its surroundings. Similar cratonic zircon ages are found in the İstanbul Paleozoic sequence (İPS) (Okay et al. 2011; Ustaömer et al. 2011), Istranca Massif (IM) (Natalin et al. 2012), and metamorphic basement rocks of the Sakarya zone (SZ) (Aysal et al. 2012; Ustaömer et al. 2016). The Neoproterozoic is represented by a total of five zircon ages between 648±17 and 999±11 Ma (Cryogenian–Tonian). Similarly, Neoproterozoic ages are reported in the İPS, IM, and metamorphic basement rocks of the SZ. The aforementioned data indicate that these "Cratonic" ages were probably derived from earlier sedimentary and/or metamorphic rocks. Peak ages yielded 545.3, 553.35, and 572.95 Ma (Ediacaran) and 494.9 and 513.45 Ma (early Cambrian), which are similar to Upper Precambrian–Cambrian magmatics, and the detrital zircon populations in sedimentary–metamorphic rocks in Turkey. Late Precambrian–Cambrian magmatism was described

in the Menderes Massif (MM) (Kroner & Şengör 1990; Bozkurt & Oberhänsli 2001; Gessner et al. 2004; Koralay et al. 2004; Bozkaya et al. 2006; Candan et al. 2011; Zlatkin et al. 2013), İstanbul zone (İZ) (Chen et al. 2002; Ustaömer et al. 2005), Armutlu peninsula (AP) (Okay et al. 2008b; Özbey et al. 2022; Sunal et al. 2022), and the IM (Yılmaz et al. 2021 and references therein). Similar zircon populations are found in the İPS (Okay et al. 2011; Ustaömer et al. 2011), IM (Natalin et al. 2012), and the underlying metamorphic rocks of the SZ (Aysal et al. 2012; Ustaömer et al. 2012, 2016). Ordovician–Silurian zircon populations are represented by peak ages of 425.25, 443.1, 458.15, 460.25, and 475.3 Ma. Ordovician magmatic rocks are described in the southern Marmara region (Okay et al. 2008a, b; Özbey et al. 2013). Okay et al. (2008a) yielded 467±4.0 Ma and 467±4.5 Ma, and Özbey et al. (2013) obtained an age of 446±8.0 Ma from jadeite-bearing metagranites south of the Izmir–Ankara–Erzincan suture belt. East of this area Okay et al. (2008b) obtained 488±6 and 457±6 Ma ages from metagranite samples intruded into amphibolite. Topuz et al. (2020) reported Silurian ages from amphibolites and metagranites in the SZ. Ordovician–Silurian zircon populations are found in the metamorphic basement of the SZ, IM, and İZ. There is no record of Ordovician–Silurian magmatic activity in the IM and the İZ. While Devonian-aged zircon populations with peak ages of 382.2 and 408.1 Ma are described in the Şile sands, this age range was not defined in the Kısırkaya region. However, Lower–Middle Devonian magmatic activity was identified within the basement rocks of the SZ (Okay et al. 2006; Aysal et al. 2012; Sunal 2012; Karslı et al. 2020; Topuz et al. 2020). Lower–Middle Devonian zircon populations were also reported in different clastic rocks within the Karakaya complex (Ustaömer et al. 2016). Carboniferous zircon populations with peak ages of 298.2, 298.55, 310.8, 311.85, 323.05, 332.15, 336.35, 341.95, 342.65, and 356.65 Ma were detected in the sands. Carboniferous zircons were measured at nine points in the Kısırkaya sands and twenty-seven points were present in the Şile sands. Carboniferous magmatism was widely described in the IM and the SZ (Ustaömer et al. 2012; Natalin et al. 2016; Topuz et al. 2019). Although Carboniferous magmatism was not identified in the İZ, significant Carboniferous zircon populations were reported in the İPS (Okay et al. 2011). The fact that there are three times more Carboniferous zircons in the Şile sands compared to the Kısırkaya region indicates that zircon may have been transported from Carboniferous magmatic rocks, especially in the SZ. Although Kısırkaya sands are very close to both the IM and the İPS, the fact that they contain less zircon is related to the relatively low input from these sources. Permian zircons are represented by peak ages of 259.7, 268.8, and 280 Ma, and there are nine zircons in the Kısırkaya sands and ten zircons in the Şile sands. Permian zircons are almost evenly distributed on both sides. Permian–Triassic magmatism was described in both the IM and the İZ (Okay et al. 2001, 2014; Sunal et al. 2006; Natalin et al. 2016; Aysal et al. 2018b and references therein). Permian magmatic rocks are also reported in the BM (Ustaömer et al. 2005; Bozkurt et al. 2012), Uludağ Massif (Topuz & Okay 2017), and the SZ (Di Rosa et al. 2019). Middle Jurassic zircons with peak ages of 155.75–161.7 Ma were found in the Kısırkaya zircons. There is no Jurassic magmatic activity defined in İstanbul. However, magmatic rocks cutting the fossiliferous Jurassic sequence were identified in the Mudurnu valley east of İstanbul (Genç & Tüysüz 2010). In addition, Middle Jurassic volcanic and plutonic rocks were dated in the Kastamonu–Küre region in the Central Pontides (Karslıoğlu Turgut et al. 2012; Okay et al. 2014). Cretaceous zircons were determined with peak ages of 71.75, 73.15, 81.55, 83.3, 98.0, 109.55, and 133.7 Ma. Upper Cretaceous volcanic rocks are defined at the base of both regions. These volcanic and plutonic rocks are present on both sides of the Bosporus with 75±2 to 67±2 Ma ages for volcanic rocks in the north of İstanbul, 67.91±0.63 to 67.59±0.5 Ma ages for the plutonic rocks (Yılmaz Şahin et al. 2012), and 72.49±0.79 to 65.44±0.93 Ma ages for the mafic-intermediate dykes cutting the İPS (Aysal et al. 2018a), and the Cretaceous zircons may have originated from these volcanic–plutonic rocks. The 56.7 Ma zircon peak ages of the Paleocene (between 63 and 56 Ma) are similar to the age of 58.9±1.8 Ma age for diorite sample (Aysal et al. 2018b) and possibly derived from similar magmatic rocks. Eocene zircons (between 56–33.9 Ma) were measured in twenty grains. Eocene volcanic–plutonic rocks crop out in large areas in the Biga Peninsula (BP) (Fig. 10), and in the AP (Harris et al. 1994; Köprübaşı & Aldanmaz 2004; Topuz et al. 2005, 2011; Okay & Satır 2006; Karacık et al. 2008; Keskin et al. 2008; Ustaömer et al. 2009; Altunkaynak et al. 2012; Sunal et al. 2019; Şen 2020). Paleocene–Eocene magmatic activity was not observed in the IM and its surroundings. However, it is noteworthy that Kısırkaya sands contain more Paleocene–Eocene zircons than the Şile sands. Oligocene–Miocene zircons were dated in the Kısırkaya and Şile sands. Oligocene–early Miocene volcanic rocks cover

Table 5: Th/Sc, Th/Co, and Th/Cr indices for the Şile and Kısırkaya sands and clays and their comparison with upper continental crust (UCC) and basic-ultrabasic abundances. (1) Cullers 1994, 2000; (2) Taylor & McLennan 1985.

Elemental ratio	Range for basic and ultrabasic source (1)	Crustal source UCC (2)	Şile Clay (n:5) average	Kısırkaya Clay (n:4) average	Şile Sandstone (n: 5) average	Kısırkaya Sandstone (n: 3) average
Th/Sc	0.05–0.22	0.79	0.660	0.415	1.929	0.559
Th/Co	0.04–1.40	0.63	1.067	0.360	4.134	0.753
Th/Cr	0.02–0.05	0.13	0.173	0.051	0.012	0.007

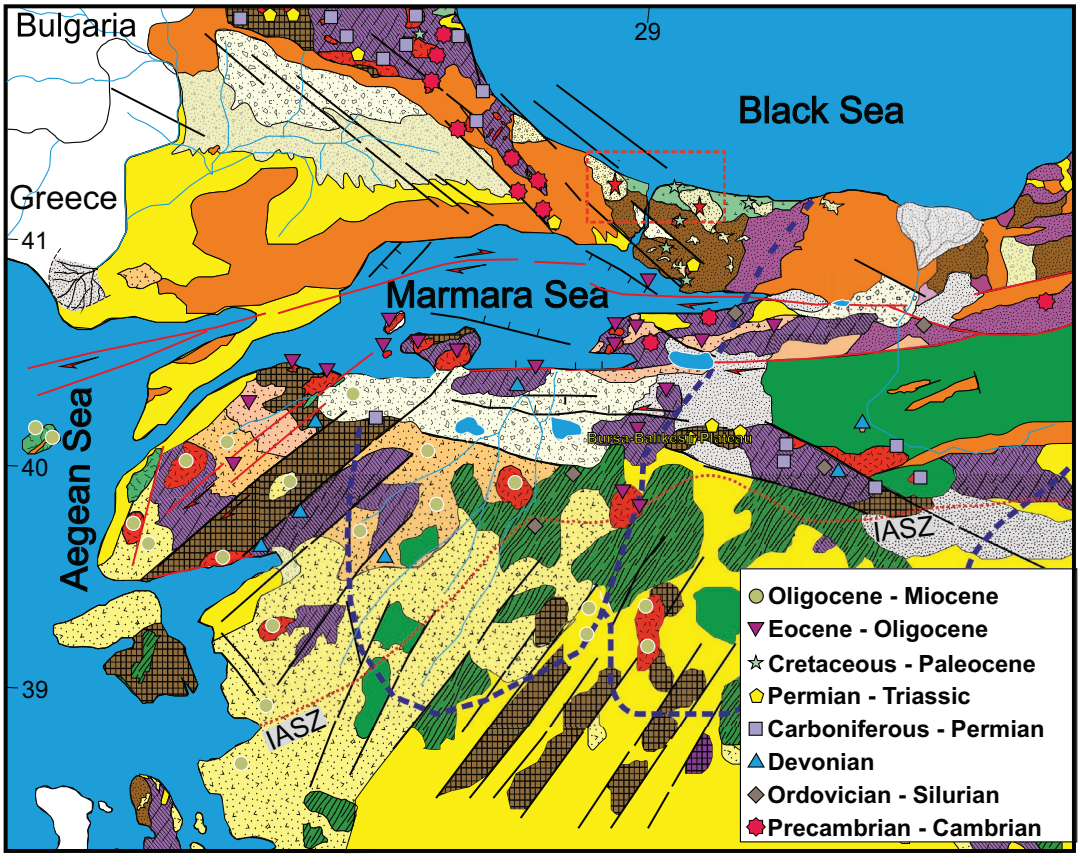

Fig. 10. Simplified geological map of NW Turkey including radiometric age data (explanations could be seen in Fig.11, references are given in the text).

a large area in the BP (Aysal 2015 and references therein). According to the findings obtained from detrital zircon ages obtained from the Kısırkaya and Şile sands, the youngest zircon age is 22.98±0.95 Ma and corresponds to the Lower Miocene Aquitanian period. The sedimentary succession that forms the Kısırkaya and Şile sands is given in Özgül et al. (2011), and it was suggested that it might be of late Oligocene–early-middle Miocene age. The data obtained show that the sedimentary sequence forming the Kısırkaya and Şile sands must be younger than the early Miocene.

Morphotectonic evolution of the İstanbul Pliocene Basin

Trace element geochemistry and zircon age data of the sands belonging to the İstanbul Pliocene show that the palaeo-river carrying the sediments derived from today's northern Aegean Sea region, passed through Çanakkale, Balıkesir, Bursa, and İstanbul, and finally discharged into the Black Sea. When the trace element values of sands and clays are normalized to the upper continental crust, the basic rock-specific elements such as Cr and Ni are above the values of the continental crust, which indicates the presence of ophiolitic rocks in this transport route and/or drainage basin. These ophiolitic rocks are Intra-Pontide or Neotethyan (İzmir–Ankara–Erzincan Suture) suture zone ophiolites.

Oligocene zircon grains in the sands revealed that the Pliocene fragments originated significantly from Çanakkale and Balıkesir regions where Oligocene volcanics exclusively cover wide areas (Dilek & Altunkaynak 2009). After the closure of the Intra-Pontide ocean at the end of the Eocene, the NW part of Anatolia uplifted because of collision and the region experienced terrestrial conditions (Yılmaz et al. 2010). This terrestrial area was further uplifted by the Oligocene pyroclastics accumulating in the Balıkesir–Çanakkale region (Altunkaynak & Yılmaz 1998; Koral et al. 2009), and the clastics originating from the high elevation area were transported to the Black Sea during the Pliocene. Rock fragmentation and decomposition in the piedmont plateau and transportation from SSW to NNE were accelerated by the structural lines extending in the NNE–SSW direction during this period. NE–SW-oriented horst and graben structures and/or drainage patterns developed in western Anatolia in the Miocene (Şengör et al. 1985; Yılmaz et al. 2000). During the Miocene and Pliocene, rivers possibly flowed from the southern plateau towards the Black Sea which existed since the late Cretaceous. Sedimentological studies also indicate the palaeocurrent direction as SW to NE for Oligocene clastics in the Thrace Basin (Elmas 2012).

At the end of the Pliocene and the beginning of the Quaternary, the Marmara Sea depression was formed by normal

faulting in E–W and NE–SW directions around Bursa and İstanbul, respectively, and the river sediments discharging into the Black Sea were blocked and then deposited along the southern shore of the Marmara Sea depression. The most typical faults that control the Marmara Sea depression and synchronous uplift of the Thrace Basin and İstanbul peninsula were related to the NE–SW trending Kartal–Tuzla fault (Eroskay & Kale 1986; Öztürk 2005), Adalar and Beykoz–Sarıyer fault (BSF) (Öztürk 1998). Beyond these three parallel normal faults, the Central Thrace fault zone (Babaeski Fault, Kırklareli Fault, Lüleburgaz Fault; Perinçek 1991; Perinçek et al. 2015) also extends in a similar direction and must have formed in the same tectonic stage. Beyond their elongation, their common features are dipping to the south and having thick terrestrial sediments in front of them. The most typical fault-bounded sediment deposits of the Quaternary occur in the Beykoz Fault where the thickness of this colluvial fan is more than 60 meters (Öztürk 1998). The vertical offset of the BSF is more than a few hundred meters, according to the displacement in the concordant Paleozoic formations. This fault caused a morphological change in the İstanbul Strait, where the İstanbul Strait undergoes a 90-degree sudden turn. The BSF crosscuts the Bosporus and extends to Sarıyer, where the Quaternary deposits have a tectonic contact with Paleozoic formations.

The BSF must have crosscut the Pliocene sediments and caused the reworking of the Pliocene clayey and sandy materials in the Quaternary. This reworked Pliocene is seen in front of the BTF and was used for tile production in both Sarıyer and Beykoz until the 1950s. Similar fault-controlled, uncemented colluvial-alluvial deposits were locally detected in İstanbul and defined as Belgrad gravels. Although there is no detailed investigation of them, some geologists stated they were Quaternary terrace deposits (Lom et al. 2016) relict from a palaeo-river system (Pamir 1938). Our investigations of this coarse-grained sedimentary succession show that they were deposited bounding the fault zone and represent a fault-controlled fan deposit. Fragmentation of the Pliocene blanket, cut by normal faults and subjected to rapid erosion and thus forming two independent Pliocene patches, remained in the east and west of the Bosporus. The Tuzla Fault is also similar to the Beykoz–Sarıyer Fault zone as it strikes in a similar direction, and also controls a linear shoreline and thick terrestrial clastic deposition in the Tuzla region (Öztürk 2005).

Pliocene river sediments, which were deposited along the Black Sea, are expected to show delta morphology on this shoreline. Contrary to a delta morphology, the NW–SE-trending linear coastal morphology is very distinctive along the Black Sea coast, which is similar to the other Quaternary fault elongations. This linear shoreline was formerly attributed to a north-dipping normal fault by Yılmaz et al. (2010), and some part of the Pliocene delta deposits must be downthrown into the Black Sea.

The low-angle normal faults which are still active and run parallel to the southern shore of the Sea of Marmara are considered detachment faults associated with core complex development and/or Uludağ uplift (Üşümezsoy 2000). This recently uplifted region is morphologically defined as the Bursa–Balıkesir Plateau (Yılmaz et al. 2010), and Bursa–Uluabat–Manyas–Gönen coastal plain (Gürer et al. 2003; Selim et al. 2012; Selim & Tüysüz 2013). These normal faults also resulted in the formation of the Sea of Marmara. On the southern side of the Marmara Sea region, many thick terrestrial alluvial sediment deposits independently occur in a large area. These formations are defined in a range from late Miocene to Holocene according to their thickness and stratigraphic positions. However, there is no certain age determination. Mostly colluvial sediments were deposited in front of the N30E-trending normal fault and outcrop on the southern slope of Kirazlıyayla Village in Yenişehir. Like the Yenişehir basin fill, Bursa and other plains include Quaternary sedimentary fill more than a few hundred metres thick.

Because of the changing tectonic regime, E–W-trending normal faults of the Marmara region began to move laterally instead of vertically. Pre-existing normal faults started to work as strike-slip faults because of changing tectonic stress. This is a phenomenon that should be expected because it is much easier to use pre-existing fractures and/or modify their movement direction instead of developing a new fracture. Therefore, most of the debate within the Sea of Marmara is due to faults that changed from old directions of movement. This is especially the case for the nature of the faults around the three deep basins in the Marmara Sea. Although there is general compressional tectonic stress, the depths of certain deeper basins in the sea of the Marmara region are possibly continuing to deepen instead of shallowing because of the activity of pre-existing normal faults opening the Marmara Sea depression. Important geological events and developments in the morphotectonic elements from Pliocene to the present in the Marmara Sea region are shown in Figure 11.

Considering that the fine clastics in the north of İstanbul were deposited in the Pliocene according to the clastic zircon ages, the formation of the Marmara Sea is the post-Pliocene event.

On the other hand, the most important structure in the Sea of Marmara is the North Anatolian Fault (NAF), which is much later than the Plio-Quaternary faults that were responsible for the opening of the Marmara region depression. The entrance of the NAF into the Sea of Marmara is generally accepted as a few hundred thousand years (İmren et al. 2001; Le Pichon et al. 2001; Şengör et al. 2005; Selim et al. 2016) Very recently, Akbayram et al. (2016) suggested an age of 3.9 million years for the entrance of the NAF into the Sea of Marmara. However, considering the Pliocene formations in the north of the Marmara Sea eliminate a few million years of formation age.

The main body of the İstanbul Pliocene river possibly flowed between two morphologically different plateaus, the Bursa and the Balıkesir plateaus, and tributaries of this river possibly met in areas within the present Sea of Marmara. This river possibly meandered in this area before reaching the İstanbul delta plain. Palaeo-river channel morphology is still seen

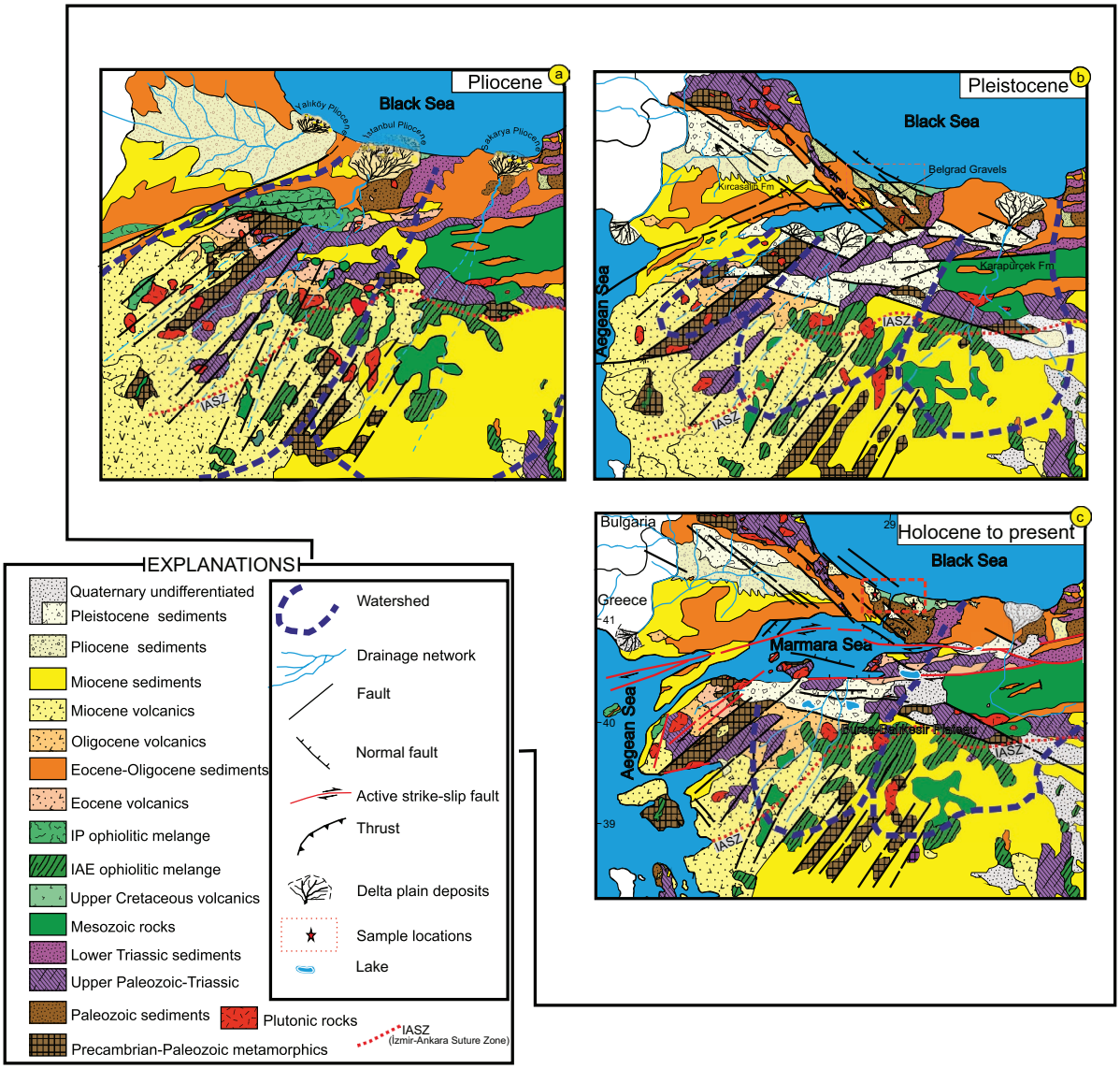

Fig. 11. Palaeogeographic map showing drainage area and transportation route of the Pliocene deltaic sediments discharging into the Black Sea (**a**), formation of the Marmara depression and blocking of the northward-flowing İstanbul Pliocene river associated with İstanbul–Thrace uplift in the north and Uludağ in the south by normal faults (**b**), entrance of the North Anatolian strike-slip fault into the Sea of Marmara, capturing of former normal faults and formation of new depressions (**c**).

under the sea of Marmara, which is a relic of the İstanbul Pliocene river (Armijo et al. 2005). It is interesting that the Bursa and Balıkesir plateau boundary, the submarine canyon in the Marmara Sea, the Bosphorus, and a major channel at the edge of the Black Sea constitute a straight line, and all must be associated with the İstanbul Pliocene river.

During the Pliocene, there must have been some other rivers flowing into the Black Sea, like the İstanbul palaeo-river. The Sakarya River is a possible relict from Pliocene time, which is locally affected by extensional tectonics in the Marmara region. Thick alluvium with a few hundred meters' thickness in the Adapazarı plain (Karapürçek Formation: Emre et al. 1998; Erturaç 2021) is related to this extensional tectonic period. However, the Sakarya River possibly quickly filled this depression and went on flowing into the Black Sea from Pliocene to the present without blockage like the İstanbul Pliocene river (Fig. 11).

Another Pliocene river was possibly the present-day Meriç (Maritsa) River, draining from the Rhodope heights and flowing into the Black Sea via the Binkılıc corridor (Elmas & Şengül 2013). Similar to the İstanbul River, the discharge from the Thrace basin into the Black Sea must have been blocked as a result of the quick uplift of the Istranca metamorphic massif in the north and/or collapse of the Thrace basin during the Quaternary period. The Pleistocene Kırcasalih Formation, which contains fault-controlled terrestrial sediments reaching a thickness of 600 meters, is the most important geological phenomenon showing the very recent uplift of

the Istranca Mountains. Due to this rapid uplift in the north and the subsidence in the south, the rivers flowing from the Thrace Basin into the Black Sea in the Pliocene turned to the south like the present Meriç–Ergene river system in the Quaternary. The Pliocene-aged terrestrial Ergene Formation with a thickness of a few km in the Thrace Basin and the terrestrial basaltic lava flows of the Miocene to Pliocene age are further evidence of a young extensional tectonic regime in the region.

Conclusion

Integrated field observations of clastic deposits, detailed geochemistry and detrital zircon U–Pb ages study conducted in the north of İstanbul to determine provenance and deposition conditions led to the following main conclusions:

- The Pliocene-aged clay, coal, and sand series occur as horizontally bedded and weakly cemented clastics which are located on the Upper Cretaceous volcano-sedimentary series in the east and west of the Bosphorus. This Pliocene sequence is represented by coarse pebble and sand at the bottom, clay and coal in the middle, and sand-rich succession at the top, and reaches a thickness of about 80 meters. They typically represent deltaic sediments.
- U/Pb ages for clay and sands obtained from zircon minerals in the sands show that the sediments originated from regions containing Neoproterozoic, Paleozoic, Mesozoic, and Oligocene formations.
- Oligocene zircon ages of the sands, trace element geochemistry of clays and sands, and regional geology indicates the source area where a palaeo-river originated from the heights of NW Anatolia and North Aegean in the Pliocene and carried sediments to the Black Sea.
- This situation reveals that the North Aegean Sea region was a piedmont plateau, subject to rapid uplift, weathering and erosion during the Pliocene.
- Pliocene rivers flowing from SSW to NNE were possibly parallel to the strike of horst-graben structures which were active in that period. Pliocene drainage basins may have been controlled by these structures.
- High Cr and Ni contents of the sand and clays, which are higher than the upper continental crust values, reveal the presence of basic-ultrabasic rocks (Neotethyan and Intra-Pontide suture zone ophiolites) in this drainage basin.
- CIA and PIA indexes of the Pliocene sediments indicate that the K-feldspar-rich magmatic rocks underwent moderate to intense weathering in the source region.
- Towards the end of the Pliocene deposition, NW–SE-trending normal faults developed in the Marmara region and resulted in the formation of the Marmara Depression as a proto-Marmara Sea between the uplifted Bursa-Balıkesir Plateau and İstanbul–Istranca Heights. During this period, the Palaeo-İstanbul river flowing into the Black Sea via İstanbul Strait must have been blocked by the Marmara Depression in the Pleistocene.
- The blocking of the Pliocene river by the Marmara Sea in the Quaternary shows that the Marmara Sea formed in the Quaternary.
- In the late Quaternary, the North Anatolian strike-slip fault entered the Marmara Sea using pre-existing normal faults within a few hundred thousand years. Our findings indicate that the Istranca Mountains also were uplifted very rapidly like the İstanbul region in the Quaternary.
- The rivers (Meriç–Ergene system) that drained from the Thrace Basin into the Black Sea were also blocked by the uplifting Istranca Mountains and turned towards the subsiding Aegean Sea. The changing of the flow direction on the Meriç river is an important research subject to clarify in future studies.

Acknowledgements: The authors thank Gözde Eren Mining company and its director Mr. Ali Karabulut for permission for the field work studies in the open pit quarry. We also thank the İstanbul University – Cerrahpaşa Research Fund unit for their support, and Prof. Dr. İlgin Kurşun, head of the Mining Engineering Department of İstanbul University – Cerrahpaşa, for their critical help with zircon separation processes. Also, we wish to thank Prof. Dr. Irena Peytcheva from the Geological Institute, Bulgarian Academy of Sciences for U–Pb zircon dating.

References

Akbayram K., Sorlien C.C. & Okay A.I. 2016: Evidence for a minimum 52±1 km of total offset along the northern branch of the North Anatolian Fault in northwest Turkey. *Tectonophysics* 668–669, 35–41.

Altunkaynak S. & Yılmaz Y. 1998: The Mount Kozak magmatic complex, western Anatolia. *Journal of Volcanology and Geothermal Research* 85, 211–231.

Altunkaynak S., Sunal G., Aldanmaz E., Genç S.C. & Dilek Y. 2012: Eocene granitic magmatism in NW Anatolia, Turkey. Revisited: New implications from comparative zircon shrimp U–Pb and ^{40}Ar–^{39}Ar geochronology & isotope geochemistry on magma genesis and emplacement. *Lithos* 155, 289–309. https://doi.org/10.1016/j.lithos.2012.09.008

Armijo R., Pondard N., Meyer B., Ucarkus G., De LBM., Malavieille J., Dominguez S., Gustcher M-A., Schmidt S., Beck C., Çağatay N., Cakir Z., Imren C., Eris K., Natalin B., Ozalaybey S., Tolun L., Lefevre I., Seeber L., Gasperini L., Rangin C., Emre O. & Sarikavak K. 2005: Submarine fault scarps in the Sea of Marmara pull-apart (North Anatolian Fault): implications for seismic hazard in Istanbul. *Geochemistry, Geophysics, Geosystems* 6, Q06009. https://doi.org/10.1029/2004GC000896

Aysal N. 2015: Mineral chemistry, crystallization conditions and geodynamic implications of the Oligo–Miocene granitoids in the Biga Peninsula, Northwest Turkey. Journal of Asian Earth Sciences 105, 68–84.

Aysal N., Ongen Öngen A.S., Peytcheva I. & Keskin M. 2012: Origin and evolution of the Havran Unit, Western Sakarya basement (NW Turkey): new LA-ICP-MS U–Pb dating of the metasedimentary–metagranitic rocks and possible affiliation to Avalonian microcontinent. *Geodinamica Acta* 25, 226–247. https://doi.org/10.1080/09853111.2014.882536

Aysal N., Keskin M, Peytcheva I. & Duru O. 2018a: Geochronology, geochemistry and isotope systematics of a mafic–intermediate dyke complex in the İstanbul Zone. New constraints on the evolution of the Black Sea in NW Turkey. *Geological Society, London, Special Publications* 464, 131–168. https://doi.org/10.1144/SP464.4

Aysal N., Yilmaz Şahin S., Gungor Güngör Y., Peytcheva I. & Ongen Öngen A.S. 2018b: Middle Permian-Early Triassic magmatism in the western Pontides, NW Turkey: Geodynamic significance for the evolution of the Paleo-Tethys. *Journal of Asian Earth Sciences* 164, 83–103.

Barka A. & Kadinsky-Cade K. 1988: Strike-slip fault geometry in Turkey and its influence on earthquake activity. *Tectonics* 7, 663–684.

Baykal F. 1942: Geology of the Şile region. *IUFF Publications, Seri B-7*, 166–233, 1–7 (in Turkish).

Baykal F. & Kaya O. 1963: General stratigraphy of Carbonifeorus in the around Istanbul. *MTA General Directorate of the Mineral Research and Exploration Publ.* 61, 1–9 (in Turkish).

Bozkaya O., Gursu Gürsu S. & Goncuoglu Göncüoğlu M.C. 2006: Textural & mineralogical evidence for a Cadomian tectonothermal event in the Eastern Mediterranean, Sandıklı-Afyon Area, western Taurides, Turkey. *Gondwana Research* 10, 301–315.

Bozkurt E. & Oberhänsli R. 2001: Menderes Massif, western Turkey: Structural, metamorphic and magmatic evolution – a synthesis. *International Journal of Earth Sciences* 89, 679–708.

Bozkurt E, Winchester J.A. & Satırir Satır M. 2012: The Çele mafic complex: Evidence for Triassic collision between the Sakarya and Istanbul Zones, NW Turkey. *Tectonophysics* 595–596, 198–214.

Büyükmeriç Y. 2015: Mediterranean-Parathetis connections from late Miocene to the present and the geological and geographical Importance of our country. *Natural Resourch and Echo. Bulletin* 20, 23–35 (in Turkish).

Candan O., Dora Ö.O., Oberhansli R., Koralay E., Çetinkaplan M., Akal C., Satır M., Chen F. & Kaya O. 2011: Stratigraphy of the Pan-African basement of the Menderes Massif & the relationship with Late Neoproterozoic/Cambrian evolution of the Gondwana. *Bulletin of the Mineral Research and Exploration Institute of Turkey* 142, 25–68.

Çelik Y., Karayiğit A.İ., Querol X., Oskay R.G., Mastaler M. & Kayseri Özer M.S. 2017: Coal characteristics, palynology, and palaeoenvironmental interpretation of the Yenikoy coal of Late Oligocene age in the Thrace Basin, NW Turkey. *International Journal of Coal Geology* 181, 103–123. https://doi.org/10.1016/j.coal.2017.08.015

Chen F., Siebel W., Satıır M., Terzioğlu N. & Saka K. 2002: Geochronology of the Karadere basement, NW Turkey and implications for the geological evolution of the İstanbul Zone. *International Journal of Earth Sciences* 91, 469–481.

Crampin S. & Evans R. 1986: Neotectonics of the Marmara Sea region of Turkey. *Journal of the Geological Society, London* 143, 343–346.

Cullers R.L. 1994: The controls on the major & trace element variation of shales, siltstones, and sandstones of Pennsylvanian–Permian age from uplifted continental blocks in Colorado to platform sediment in Kansas, USA. *Geochimica et Cosmochima Acta* 58, 4955–4972.

Cullers R.L. 2000: The geochemistry of shales, siltstones and sandstones of Pennsylvanian–Permian Age, Colorado, U.S.A.: implications for provenance and metamorphic studies. *Lithos* 51, 181–203. https://doi.org/10.1016/S0024-4937(99)00063-8

Depetris P.J., Pasquinii A.I & Lecomte K.l. 2014: Weathering and the riverine denudation of continents. Springer Briefs in Earth System Sciences, South America and the Southern Hemisphere. *Springer*, Dordrecht, 1–93.

Di Rosa M., Farina F., Marroni M., Pandolfi L., Göncüoğlu M.C., Ellero A. & Ottria G. 2019: U–Pb zircon geochronology of intrusive rocks from an exotic block in the Late Cretaceous–Paleocene Tarakli Flysch (northern Turkey): constraints on the tectonics of the Intrapontide suture zone. *Journal of Asian Earth Sciences* 171, 277–288.

Dilek Y. & Altunkaynak Ş. 2009: Geochemical and temporal evolution of Cenozoic magmatism in western Turkey: mantle response to collision, slab break-off, and lithospheric tearing in an orogenic belt. *Geological Society, London, Special Publications* 311, 213–233.

Ece Ö.I., Nakagawa Z.E. & Schroeder P.A. 2003: Alteration of volcanic rocks and genesis of kaolin deposits in the Sile region, northern Istanbul, Turkey. Part – I. Clay Mineralogy. *Clays and Clay Minerals* 51, 675–688.

Elmas M.A. 2012: The Thrace Basin: stratigraphic and tectonic-palaeogeographic evolution of the Palaeogene formations of northwest Turkey. *International Geology Review* 54, 1419–1442.

Elmas M.A. & Şengül A. 2013: Miocene formations and NE-trending right-lateral strike–slip tectonism in Thrace, northwest Turkey: geodynamic implications. *International Geology Review* 55, 705–729.

Emre Ö., Erkal T., Tchepalyga A., Kazancı N., Keçer M. & Unay E. 1998: Neogene–Quaternary evolution of eastern Marmara region, nortwest Turkey. *Bulletin of the Mineral Research and Exploration Institute of Turkey* 120, 119–145.

Eroskay O. & Kale S. 1986: İstanbul Boğazı Tüp Geçişi Güzergahında jeoteknik bulgular. *Mühendislik Jeolojisi Bülteni* 8, 2–7 (in Turkish).

Erturaç M.K. 2021: Late Pleistocene–Holocene characteristics of the North Anatolian Fault at Adapazarı Basin: evidence from the age and geometry of the fluvial terrace staircases. *Turkish Journal of Earth Sciences* 30, 93–115.

Fedo C.M., Eriksson K.A. & Krogstad E.J. 1996: Geochemistry of shales from the Archean (similar to 3.0 Ga) Buhwa greenstone belt, Zimbabwe: Implications for provenance and source-area weathering. *Geochimica et Cosmochimica Acta* 60, 1751–1763.

Fedo C.M., Nesbitt H.W. & Young G.M. 1995: Unraveling the effects of potassium metasomatism in sedimentary-rocks and paleosols, with ımplications for paleoweathering conditions and provenance. *Geology* 23, 921–924.

Feng R. & Kerrich R. 1990: Geochemistry of Fine Grained Clastic Sediments in the Archaean Abitibi Greenstone Belt, Canada: Implications for Provenance and Tectonic Setting. *Geochimica et Cosmochimica Acta* 54, 1061–1081.

Floyd P.A. & Leveridge B.E. 1987: Tectonic environment of the Devonian Gramscatho Basin, South Cornwall: framework mode and geochemical evidence from turbiditic sandstones. *Journal of the Geological Society* 144, 531–542.

Gedik I., Duru M., Pehlivan Ş. & Timur E. 2005: Geological maps of Turkey Istanbul G22b3 sheet, 11-13. *MTA General Directorate of the Mineral Research and Exploration*.

Genç S.C. & Tüysüz O. 2010: Tectonic setting of the Jurassic bimodal magmatism in the Sakarya Zone (Central and Western Pontides), Northern Turkey: A geochemical and isotopic approach. *Lithos* 118, 95–111. https://doi.org/10.1016/j.lithos.2010.03.017

Gessner K., Collins A.S., Ring U. & Güngör T. 2004: Structural and thermal history of poly-orogenic basement: U–Pb geochronology of granitoid rocks in the southern Menderes Massif, western Turkey. *Journal of the Geological Society* 161, 93–101.

González-Álvarez I. & Kerrich R. 2012: Weathering intensity in the Mesoproterozoic & modern large-river systems: a comparative study in the Belt-Purcell Supergroup, Canada and USA. *Precambrian Research* 208–211, 174–196. https://doi.org/10.1016/j.precamres.2012.04.008

Görür N., Cagatay M.N., Sakınç M., Sümengen M., Sentürk K., Yaltirak C. & Tchapalyga A. 1997: Origin of the Sea of Marmara as deduced from Neogene to Quaternary paleogeographic evolution of its frame. *International Geology Review* 39, 342–352.

Guillong M., Meier D.L., Allan M.M., Heinrich C.A. & Yardley B.W.D. 2008: SILLS: A MATLAB-based program for the reduction of laser ablation ICP-MS data of homogeneous materials and inclusions. In: Sylvester P. J. (Ed.): Laser Ablation ICP-MS in the Earth Sciences: Current Practices and Outstanding Issues. *Mineralogical Association of Canada Short Course* 40, 328–333. .

Gürer Ö.F., Kaymakçı N., Çakır S. & Özburan M. 2003: Neotectonics of the southeast Marmara Region, NW Anatolia, Turkey. *Journal of Asian Earth Sciences* 21, 1041–1051.

Harris N.B.W., Kelley S. & Okay A.I. 1994: Post-collisional magmatism and tectonics in northwest Anatolia. *Contributions to Mineralogy and Petrology* 117, 241–252.

İmren C., Le Pichon X., Rangin C., Demirbağ E. & Ecevitoğlu B. 2001: The North Anatolian Fault within the Sea of Marmara: a new interpretation based on multi-channel seismic and multi-beam bathymetry data. *Earth and Planetary Science Letters* 186, 143–158.

Karacık Z., Yılmaz Y., Pearce J.A. & Ece Ö.I. 2008: Petrochemistry of the south Marmara Granitoids, Northwest Anatolia, Turkey. *International Journal of Earth Sciences* 97, 1181–1200.

Karslı O., Şengün F., Dokuz A., Kandemir R., Aydın F. & Andersen T. 2020: Silurian to Early Devonian arc magmatism in the western Sakarya Zone (NW Turkey), with inference to the closure of the Rheic Ocean. *Lithos* 370–371, 105641. https://doi.org/10.1016/j.lithos.2020.105641

Karslıoğlu Turgut O., Ustaömer T., Robertson A.H. & Peytcheva I. 2012: Age and provenance of detrital zircons from a sandstone turbidite of the Late Triassic–Early Jurassic Küre Complex, Central Pontides, N Turkey. *International Earth Science Colloquium on the Aegean Region*, İzmir, Turkey, 1–57.

Keskin M., Ustaömer T. & Yeniyol M. 2003: Stratigraphy, petrology and tectonic environment of Upper Cretaceous volcano-sedimentary units cropping out at the North of Istanbul. In: Gungor Y. (Ed.): Proceedings of the Geology of Istanbul Symposium. *Turkish Chamber of Geological Engineers*, Istanbul, 23–35.

Keskin M., Genç S.C. & Tüysüz O. 2008: Petrology and geochemistry of post-collisional Middle Eocene volcanic units in North-Central Turkey: Evidence for magma generation by slab breakoff following the closure of the Northern Neotethys Ocean. *Lithos* 104, 267–305. https://doi.org/10.1016/j.lithos.2007.12.011

Köprübaşı N. & Aldanmaz E. 2004: Geochemical constraints on the petrogenesis of Cenozoic I-Type granitoids in northwestern Anatolia, Turkey: evidence for magma generation by lithospheric delamination in post-collisional setting. *International Geology Review* 46, 705–729. https://doi.org/10.2747/0020-6814.46.8.705

Koral H., Öztürk H. & Hanilçi N. 2009: Tectonically induced coastal uplift mechanism of Gokceada Island, Northern Aegean Sea, Turkey. *Quaternary International* 197, 43–54.

Koralay E., Dora O.Ö., Chen F., Satır M. & Candan O. 2004: Geochemistry and geochronology of orthogneisses in the Derbent (Alaşehir) area, eastern part of the Ödemiş–Kiraz Submassif, Menderes Massif: Pan-African magmatic activity. *Turkish Journal of Earth Sciences* 13, 37–61.

Kroner A. & Şengör A.M.C. 1990: Archean and Proterozoic ancestry in Late Precambrian to Early Paleozoic crustal elements of southern Turkey as revealed by single-zircon dating. *Geology* 18, 1186–1190.

Le Pichon X., Şengör A.M.C., Demirbağ E. Rangin C., Imren C., Armijo R., Görür N., Çağatay N., De Lepinay B.M., Meyer B., Saatçılar R. & Tok B. 2001: The active main Marmara Fault. *Earth and Planetary Science Letters* 192, 595–616.

Le Pichon X., Chamot-Rooke N., Rangin C. & Şengör A.M.C. 2003: The North Anatolian fault in the Sea of Marmara. *Journal of Geophysical Research* 108, published online 2 April 2003. https://doi.org/10.1029/2002JB001862

Linnemann U., Ouzegane K., Drareni A., Hofmann M., Becker S., Gärtner A. & Sagawe A. 2011: Sands of west Gondwana: an archive of secular magmatism and plate interactions – a case study from the Cambro–Ordovician section of the Tassili Ouan Ahaggar (Algerian Sahara) using U–Pb LA-ICP-MS detrital zircon ages. *Lithos* 123, 188–203. https://doi.org/10.1016/j.lithos.2011.01.010

Lom N., Ülgen S.C., Sakınç M. & Şengör A.M.C. 2016: Geology and stratigraphy of Istanbul region. *Geodiversitas* 38, 175–195. https://doi.org/10.5252/g2016n2a3

McLennan S.M. 2001: Relationship between the trace element composition of sedimentary rocks and upper continental crust. *Geochemistry, Geophysics, Geosystems* 2, 2000GC000109. https://doi.org/10.1029/2000GC000109

McLennan S.M., Hemming S., McDaniel D.K. & Hanson G.N. 1993: Geochemical approaches to sedimentation, provenance, and tectonics. In: Johnson M.J. & Basu A. (Eds.): Processes Controlling the Composition of Clastic Sediments. *Geological Society of America Special*, 21–40.

Mongelli G., Critelli S., Perri F., Sonnino M. & Perrone V. 2006: Sedimentary recycling, provenance and paleoweathering from chemistry and mineralogy of Mesozoic continental redbed mudrocks, Peloritani Mountains, Southern Italy. *Geochemical Journal* 40, 197–209.

Natalin B.A., Sunal G., Satır M. & Toraman E. 2012: Tectonics of the Istranca Massif, NW Turkey: History of a long-lived arc at the northern margin of Paleo-Tethys. *Turkish Journal of Earth Sciences* 21, 755–798.

Natalin B.A., Sunal G., Gun E., Wang B. & Zhiqing Y. 2016: Precambrian to Early Cretaceous rocks of the Strandja Massif (northwestern Turkey): evolution of a long lasting magmatic arc. *Canadian Journal of Earth Sciences* 53, 1312–1335.

Nesbitt H.W. & Young G.M. 1984: Prediction of some weathering trends of plutonic and volcanic rocks based on thermodynamic and kinetic considerations. *Geochimica et Cosmochimica Acta* 48, 1523–1534.

Okay A.I. 1989: Tectonic units and sutures in the Pontides, northern Turkey. In: Şengör A.M.C. (Ed.): Tectonic Evolution of the Tethyan Region. *NATO Advanced ASI Series, Kluwer Academic Publications*, Dordrecht, 109–116.

Okay A. & Satır M. 2006: Geochronology of Eocene plutonism and metamorphism in northwest Turkey: evidence for a possible magmatic arc. *Geodinamica Acta* 19, 251–266.

Okay A.I., Tansel I. & Tüysüz O. 2001: Obduction, subduction and collision as reflected in the Upper Cretaceous–Lower Eocene sedimentary record of western Turkey. *Geological Magazine* 138, 117–142.

Okay A.I., Satır M. & Siebel W. 2006: Pre-Alpide orogenic events in the Eastern Mediterranean region. In: Gee D.G. & Stephenson R.A. (Eds.): European Lithosphere Dynamics. *Geological Society, London, Memoirs* 32, 389–405.

Okay A.I., Satır M. & K. Shang C. 2008a: Ordovician metagranitoid from the Anatolide–Tauride Block northwest Turkey: geodynamic implications. *Terra Nova* 20, 380–288. https://doi.org/10.1111/j.1365-3121.2008.00818.x

Okay A.I., Bozkurt E., Satır M., Yigitbaş E., Crowley Q.G. & K. Shang C. 2008b: Defining the southern margin of Avalonia in the Pontides: geochronological data from the Late Proterozoic and Ordovician granitoids from NW Turkey. *Tectonophysics* 461, 252–264. https://doi.org/10.1016/j.tecto.2008.02.004

Okay A.I., Sunal G., Tüysüz O., Sherlock S., Keskin. M. & Kylander-Clark A.R.C. 2014: Low-pressure–high-temperature metamorphism during extension in a Jurassic magmatic arc, central Pontides, Turkey. *Journal of Metamorphic Geology* 32, 49–69.

Okay A.I., Özcan E., Hakyemez A., Siyako M., Sunal G. & Kylander-Clark A.R.C. 2019: The Thrace Basin and the Black Sea: The Eocene–Oligocene connection. *Geological Magazine* 156, 39–61. https://doi.org/10.1017/S0016756817000772

Okay N., Zack T., Okay A.I. & Bart M. 2011: Sinistral transport along the Trans-European Suture Zone: detrital zircon–rutile geochronology and sandstone petrography from the Carboniferous flysch of the Pontides. *Geological Magazine* 148, 380–403. https://doi.org/10.1017/S0016756810000804

Önalan M. 1981a: Geology and sedimentary Characteristics of Pendik region and Islands. Istanbul University, Faculty of Earth sciences. *Dissertation Thesis*, İstanbul 1–193 (in Turkish).

Önalan M. 1981b: The depositional environments of the Istanbul Ordovician and Silurian deposits. *Istanbul Journal of Earth Sciences* 2, 161–177 (in Turkish).

Özbey Z., Ustaömer T., Robertson A.H.F. & Ustaömer P.A. 2013: Tectonic significance of Late Ordovician granitic magmatism and clastic sedimentation on the northern margin of Gondwana (Tavsanli Zone, NW Turkey). *Journal of the Geological Society* 170, 159–173.

Özbey Z., Karslıoğlu Ö. & Aysal N. 2022: First evidence for the subduction initiation and boninitic magmatism from the Armutlu Peninsula (NW Turkey): geodynamic significance for the Cadomian magmatic arc system of the Gondwanan margin. *International Geology Review* 64, 2497–2521. https://doi.org/10.1080/00206814.2021.1986680

Özgül N., Özcan I., Akmeşe I., Üner K., Bilgin I., Korkmaz R., Yıldırım U., Yıldız Z., Akdağ Ö. & Tekin M. 2011: Geology of the Istanbul city. *Istanbul Metropolitan Municipality*, 1–305 (in Turkish).

Öztürk H. 1998: Geology of Beykoz (Istanbul, Turkey) area and evidences for the development of Istanbul Strait. *Istanbul Journal of Earth Sciences* 10, 1–11 (in Turkish with English abstract).

Öztürk H. 2005: Metropolitan development on drought history of the Tuzla Lake, Istanbul, Turkey. *Journal of Coastal Research* 21, 255–262.

Pamir H.N. 1938: The issue of the formation of the Bosphorus. *Bulletin of the Mineral Research and Exploration Institute of Turkey* 13, 61–69 (in Turkish).

Paul D., White W.M. & Turcotte D.L. 2003: Constraints on the $^{232}Th/^{238}U$ ratio (K) of the continental crust. *Geochemistry, Geophysics, Geosystems* 4, 1102.

Perinçek D. 1991: Possible strand of the North Anatolian Fault in the Thrace Basin, Turkey – An Interpretation. *AAPG Bulletin* 75, 241–257.

Perinçek D., Ataş N., Karatut S. & Erensoy E. 2015: Geological factors controlling potential of lignite beds within the danişmen formation in the Thrace Basin. *Bulletin of the Mineral Research and Exploration Institute of Turkey* 150, 79–110 (in Turkish with English abstract).

Popov S.V., Shcherba I.G., Ilyina L.B., Nevesskaya L.A., Paramonova N.P., Khondkarian S.O. & Magyar I. 2006: Late Miocene to Pliocene palaeogeography of the Paratethys and its relation to the Mediterranean. *Palaeogeography, Palaeoclimatology, Palaeoecology*, 238, 91–106.

Price J.R. & Velbel M.A. 2003: Chemical weathering indices applied to weathering profiles developed on heterogenous felsic metamorphic parent rocks. *Chemical Geology* 202, 397–416. https://doi.org/10.1016/j.chemgeo.2002.11.001

Pruett R.J. 2016: Kaolin deposits and their uses: Northern Brazil and Georgia, USA. *Applied Clay Science* 131, 3–13. https://doi.org/10.1016/j.clay.2016.01.048

Roddaz M., Viers J., Brusset S., Baby P., Bouceyrand C. & Herail G. 2006: Controls on weathering and provenance in the Amazonian Foreland Basin: insights from major and trace element geochemistry of Neogene Amazonian Sediments. *Chemical Geology* 226, 31–65.

Rögl F. 1998: Palaeogeographic Considerations for Mediterranean and Paratethys Seaways (Oligocene to Miocene). *Annalen des Naturhistorischen Museums in Wien* 99A, 279–310.

Roser B.P. & Korsch R.J. 1988: Provenance signatures of sand stone-mudstone suites determined using discriminant function analysis of major element data. *Chemical Geology* 67, 119–139.

Sayar C. 1964: Ordovician Conularids from the Bosphorus Area, Turkey. *Geological Magazine* 101, 193–197. https://doi.org/10.1017/S0016756800049438

Selim H.H. & Tüysüz O. 2013: The Bursa–Gönen Depression, NW Turkey: A complex basin developed on the North Anatolian Fault. *Geological Magazine* 150, 801–821. https://doi.org/10.1017/S0016756812000945

Selim H.H., Tüysüz O., Karakaş A. & Taş K.O. 2012: Morphotectonic evidence from the southern branch of the North Anatolian Fault (NAF) and basins of the south Marmara Sub-Region, NW Turkey. *Quaternary International*, published Online 23 November 2012. https://doi.org/10.1016/J.Quaint.2012.11.022

Selim H.H., Yavuz O., Gürer O.F., Karakaş A. & Taş K.O. 2016: Age determination for segments of the North Anatolian Fault (NAF) northern branch by $^{234}U/^{230}Th$ dating of Soğucak (Yalova) range-front travertines, south Marmara, Turkey. *Quaternary International* 425, 416–424.

Şen F. 2020: Middle Eocene high-K acidic volcanism in the Princes' Islands (İstanbul) and its geodynamic implications. *Turkish Journal of Earth Sciences* 29, 208–219.

Şengör A.M.C. 2011: Why was the Istanbul strait opened in the Bosphorus? *Physical Geography Research, Turkish Geographical Society* 5, 57–102 (in Turkish).

Şengör A.M.C & Yılmaz Y. 1981: Tethyan Evolution of Turkey: A Plate Tectonic Approach. *Tectonophysics* 75, 181–241. https://doi.org/10.1016/0040-1951(81)90275-4

Şengör A.M.C., Görür N. & Şaroğlu F. 1985: Strike-slip faulting and related basin formation in zones of tectonic escape: Turkey as a case study. In: Biddle K.T. & Blick N.C. (Eds.): Strike-slip deformation, Basin Formation and Sedimentation. *Society of Economic Palaeontologists and Mineralogists, Special Publications* 37, 227–264.

Şengör A.M.C., Tüysüz O., İmren C., Sakınç M., Eyidoğan H., Görür N., Le Pichon X. & Ranging C. 2005: The North Anatolian Fault: a new look. *Annual Review of Earth and Planetary Sciences* 33, 37–112.

Siyako M. 2006: Lithostratigraphy units of Thrace Region (Tertiary Part) Stratigraphy Committee. Lithostratigraphy unit series-2, *Mineral Research and Exploration Institute of Turkey*, 1–70 (in Turkish).

Sun S.S. & McDonough W.F. 1989: Chemical and isotopic systematics of oceanic basalts: implications for mantle composition and processes. In: Saunders A. D. & Norry M.J. (Eds): Magmatism in the ocean basins. *Geological Society London, Special Publication* 42, 313–345.

Sunal G. 2012: Devonian magmatism in the western Sakarya Zone, Karacabey Region, NW Turkey. *Geodinamica Acta* 25, 183–201.

Sunal G., Natalin B.A., Satır M. & Toraman E. 2006: Palaeozoic magmatic events in the Istranca Massif, NW Turkey. *Geodinamica Acta* 19, 281–298.

Sunal G., Erturaç M.K., Topuz G., Okay A.I. & Zack T. 2019: The Early Eocene Ekmekçi granodiorite porphyry in the Karacabey Region (Sakarya Zone, NW Turkey). *Turkish Journal of Earth Sciences* 28, 589–602.

Sunal G., Akın A., Erturaç M.K., Ay C. & Dunkle I. 2022: Paleo-exhumation histories of the Sakarya and the Istanbul Zones of the Western Pontides, the Almacık Block and its surroundings, NW Turkey. *International Geology Review*. https://doi.org/10.1080/00206814.2022.2084645

Taylor S.R. & McLennan S.M. 1985: The continental crust: its composition and evolution. *Blackwell Scientific Publications*, Oxford, 1–312.

Teipel U., Eichhorn R., Loth G., Rohrmuller J., Holl R. & Kennedy A. 2004: U–Pb Shrimp and Nd isotopic data from the western Bohemian Massif (Bayerischer Wald, Germany): Implications for Upper Vendian and Lower Ordovician magmatism. *International Journal of Earth Sciences* 93, 782–801.

Topuz G. & Okay A.I. 2017: Late Eocene–early Oligocene two-mica granites in NW Turkey (the Uludağ Massif): water-fluxed melting products of a mafic metagreywacke. *Lithos* 268, 334–350.

Topuz G., Altherr R., Schwarz W.H., Siebel W., Satır M. & Dokuz A. 2005: Post-collisional plutonism with adakite-like signatures: The Eocene Saraycık Granodiorite (Eastern Pontides, Turkey). *Contributions to Mineralogy and Petrology* 150, 441–455.

Topuz G., Okay A.I., Altherr R., Schwarz W.H., Siebel W., Satir M. & Dokuz A. 2011: Post-collisional adakite-like magmatism in the Ağvanis Massif and implications for the evolution of the Eocene magmatism in the Eastern Pontides (NE Turkey). *Lithos* 125, 131–150. https://doi.org/10.1016/j.lithos.2011.02.003

Topuz G., Candan O., Zack T., Chen F. & Li Q.L. 2019: Early Miocene high-potassium I-type granite plutonism in the East Anatolian plateau (the Taşlıçay intrusion). *Lithos* 348, 105210. https://doi.org/10.1016/j.lithos.2019.105210

Topuz G., Candan O., Okay A.I., Quadt A., Othman M., Zack T. & Wang J. 2020: Silurian anorogenic basic and acidic magmatism in northwest Turkey: Implications for the opening of the Paleo-Tethys. *Lithos* 356, 105302. https://doi.org/10.1016/j.lithos.2019.105302

Turgut S. & Eseller G. 2000: Sequence Stratigraphy, tectonics and depositional history in eastern Thrace Basin, NW Turkey. *Marine and Petroleum Geology* 17, 61–100.

Ülgen S., Lom N., Sunal G., Gerdes A. & Şengör A.M.C. 2018: The Strandja Massif and the İstanbul Zone were once parts of the same palaeotectonic unit: new data from Triassic detrital zircons. *Geodinamica Acta* 30, 212–224.

Ustaömer P.A., Mundil R. & Renne P.R. 2005: U/Pb and Pb/Pb Zircon ages for arc-related intrusions of the Bolu Massif (W Pontides, NW Turkey): Evidence for late Precambrian (Cadomian) Age. *Terra Nova* 17, 215–223

Ustaömer P.A., Ustaömer T., Collins A.S. & Reischpeitsch J. 2009: Lutetian arc-type magmatism along the Southern Eurasian Margin: New U–Pb La-ICP MS and whole-rock geochemical data from Marmara Island, NW Turkey. *Mineralogy and Petrology* 96, 177–196.

Ustaömer P.A., Ustaömer T., Gerdes A. & Zulauf G. 2011: Detrital zircon ages from a Lower Ordovician quartzite of the Istanbul Exotic Terrane (NW Turkey): Evidence for Amazonian affinity. *International Journal of Earth Sciences (Geologische Rundschau)* 100, 23–41.

Ustaömer P.A., Ustaömer T. & Robertson A.H.F. 2012: Ion Probe U–Pb Dating of the Central Sakarya Basement: A Peri-Gondwana terrane intruded by Late Lower Carboniferous subduction/collision-related granitic rocks. *Turkish Journal of Earth Sciences* 21, 905–932.

Ustaömer T., Ustaömer P.A., Robertson A.H.F. & Gerdes A. 2016: Implications of U–Pb and Lu–Hf Isotopic analysis of detrital zircons for the depositional age, provenance and tectonic setting of the Permian–Triassic Palaeotethyan Karakaya Complex, NW Turkey. *International Journal of Earth Sciences* 105, 7–38.

Üşümezsoy S. 2000: Seismic analyse of the detachment tectonic in the Sea of Marmara. In: Ozturk B., Kadıoğlu M. & Ozturk H. (Eds.): Marmara Denizi 2000 Symposium, Proceeding Book. *Tüdav Publication* 5, 248–259.

Vermesch P. 2018: IsoplotR: a free and open toolbox for geochronology. *Geoscience Frontiers* 9, 1479–1493.

Walker J.D., Geissman J.W., Bowring S.A. & Babcock L.E. 2018: Geologic Time Scale v. 5.0. *Geological Society of America*.

Walter B.L., Walter C.W., Raymond M.T. & Elizabeth F.O. 1965: Bauxite and kaolin deposits of the Irwinton District Georgia. *USGS Bulletin* 1199-J, 26.

Yalçın M.N. & Yılmaz İ. 2010: Devonian in Turkey – a review. *Geologica Carpathica* 61, 235–253.

Yeniyol M. 1984: Occurence of clays of Istanbul. *Bulletin of Geological Society Turkey* 5, 143–150 (in Turkish).

Yılmaz İ, Yılmaz Şahin S, Aysal N, Güngör Y, Akgündüz A.& Bayhan U.C. 2021: Geochronology, geochemistry and tectonic setting of the Cadomian (Ediacaran–Cambrian) magmatism in the Istranca (Strandja) Massif: new insights into magmatism along the northern margin of Gondwana in NW Turkey. *International Geology Review* 64. https://doi.org/10.1080/00206814.2021.1901249

Yılmaz Şahin S., Aysal N. & Güngör Y. 2012: Petrogenesis of Late Cretaceous adakitic magmatism in the İstanbul Zone (Çavuşbaşı Granodiorite, NW Turkey). *Turkish Journal of Earth Sciences* 21, 1029–1045.

Yılmaz Şahin S., Aysal N., Güngör Y., Peytcheva I. & Neubauer F. 2014: Geochemistry and U–Pb Zircon Geochronology of Metagranites in Istranca (Strandja) Zone, NW Pontides, Turkey: Implications for the geodynamic evolution of Cadomian Orogeny. *Gondwana Research* 26, 755–771.

Yılmaz Y., Genç S. C., Gürer Ö.F., Bozcu M., Yılmaz K., Karacık Z., Altunkaynak & Elmas A. 2000: When did the western Anatolian grabens begin to develop? *Geological Society London, Special Publications* 173, 353–384.

Yılmaz Y., Gökaşan E. & Erbay A.Y. 2010: Morphotectonic development of the Marmara Region. *Tectonophysics* 488, 51–70.

Zlatkin O., Avigad D. & Gerdes A. 2013: Evolution and provenance of Neoproterozoic basement and Lower Paleozoic siliciclastic cover of the Menderes Massif (Western Taurides): Coupled U–Pb–Hf zircon isotope geochemistry. *Gondwana Research* 23, 682–700.

Electronic supplementary material is available online:

Supplementary Table S1 at http://geologicacarpathica.com/data/files/supplements/GC-74-1-Ozturk_Suppl_Table_S1.xlsx
Supplementary Table S2 at http://geologicacarpathica.com/data/files/supplements/GC-74-1-Ozturk_Suppl_Table_S2.xlsx